

Digital Filter Design using LMI Based Techniques

by

Wasim Mohamed Munther Al-Baroudi

A Thesis Presented to the

FACULTY OF THE COLLEGE OF GRADUATE STUDIES

KING FAHD UNIVERSITY OF PETROLEUM & MINERALS

DHAHRAN, SAUDI ARABIA

In Partial Fulfillment of the
Requirements for the Degree of

MASTER OF SCIENCE

In

SYSTEMS ENGINEERING

June, 1997

INFORMATION TO USERS

This manuscript has been reproduced from the microfilm master. UMI films the text directly from the original or copy submitted. Thus, some thesis and dissertation copies are in typewriter face, while others may be from any type of computer printer.

The quality of this reproduction is dependent upon the quality of the copy submitted. Broken or indistinct print, colored or poor quality illustrations and photographs, print bleedthrough, substandard margins, and improper alignment can adversely affect reproduction.

In the unlikely event that the author did not send UMI a complete manuscript and there are missing pages, these will be noted. Also, if unauthorized copyright material had to be removed, a note will indicate the deletion.

Oversize materials (e.g., maps, drawings, charts) are reproduced by sectioning the original, beginning at the upper left-hand corner and continuing from left to right in equal sections with small overlaps. Each original is also photographed in one exposure and is included in reduced form at the back of the book.

Photographs included in the original manuscript have been reproduced xerographically in this copy. Higher quality 6" x 9" black and white photographic prints are available for any photographs or illustrations appearing in this copy for an additional charge. Contact UMI directly to order.

UMI

A Bell & Howell Information Company
300 North Zeeb Road, Ann Arbor MI 48106-1346 USA
313/761-4700 800/521-0600

NOTE TO USERS

The original manuscript received by UMI contains pages with slanted print. Pages were microfilmed as received.

This reproduction is the best copy available

UMI



DIGITAL FILTER DESIGN USING LMI BASED TECHNIQUES

BY

WASIM MOHAMED MUNTHAR AL-BAROUDI

A Thesis Presented to the
FACULTY OF THE COLLEGE OF GRADUATE STUDIES
KING FAHD UNIVERSITY OF PETROLEUM & MINERALS
DHAHRAN, SAUDI ARABIA

In Partial Fulfillment of the
Requirements for the Degree of

MASTER OF SCIENCE
In

SYSTEMS ENGINEERING

JUNE 1997

UMI Number: 1391781

UMI Microform 1391781
Copyright 1998, by UMI Company. All rights reserved.

**This microform edition is protected against unauthorized
copying under Title 17, United States Code.**

UMI
300 North Zeeb Road
Ann Arbor, MI 48103

KING FAHED UNIVERSITY OF PETROLEUM AND MINERALS
DHAHRAN 31261, SAUDI ARABIA

COLLEGE OF GRADUATE STUDIES

This thesis, written by **WASIM MOHAMED MUNTHAR AL BAROUDI** under the direction of his Thesis Advisor and approved by his Thesis Committee, has been presented to and accepted by the dean of the College of Graduate Studies, in partial fulfillment of the requirements for the degree of MASTER OF SCIENCE, IN SYSTEMS ENGINEERING.

Thesis Committee

Dr. Davut Kavranoglu
D. Kavranoglu 26/1/1998
Thesis Advisor

Md. Shafiq Ahmed
Member

Dr. N. Bettaieb
Member

[Signature]
Department Chairman

M. Elsh. [Signature]
Member

[Signature]
Dean, College of Graduate Studies



[Signature]
Member

7/6/98
Date

Dedicated to

My Mother and Father

ACKNOWLEDGEMENTS

Praise be to the Lord of the World, the Almighty for having guided me at every stage of my life.

I have been fortunate to have the opportunity to work under the supervision of Dr. Davut Kavranoglu. His guidance, valuable suggestions and support throughout all stages of my thesis are highly appreciated. I would also like to place on record my appreciation for the cooperation and guidance extended by my committee members, Prof. M. S. Ahmed, Dr. Maamar Bettayeb, Dr. Mostafa El-Shafei and Dr. Shukri Selim.

I also thank my friends Mr. Farooq Anjum and Mr. Husni Mohtasib, who have been a source of great help during my M.S. I am grateful to all my friends, both from within and outside the department, who made my stay at KFUPM a pleasant and memorable one.

I recall with deep gratitude and respect the debt I owe to my mother, father and brothers for their unfathomable love, prays, support and encouragement throughout my studies. I would also like to thank my wife for the support and patience she extended during my thesis. May Allah bless them all.

CONTENTS

Acknowledgements	i
List of Figures	iv
List of Tables	vii
Abstract (English)	viii
Abstract (Arabic)	ix

1 INTRODUCTION

1.1 Literature Survey	1
1.2 Scope of Work	7
1.2.1 L_∞ Optimal FIR Filter Design Problem	7
1.2.2 L_∞ Optimal IIR Filter Design Problem	8
1.2.3 Optimal Power Spectrum Approximation Problem (IIR/FIR)	8
1.3 Organization	10

2 PRELIMINARIES

2.1 Basics of LMI Based Optimization Techniques	11
2.2 Filter Design Techniques	13
2.2.1 Filter Design Problem	14
2.2.2 FIR Filter Design	15
2.2.3 IIR Filter Design	17
2.3 Power Spectrum Estimation	20
2.4 Characterization of the Solution of L_∞ Norm Approximation	22
2.4.1 L_∞ Approximation Problem (SISO Systems)	22

3 LMI-Based Filter Design

3.1 L_∞ Optimal Filter Design Problem	24
--	----

3.1.1 The Problem	24
3.2 The FIR Case	28
3.3 The IIR Case	31
3.4 FIR-Based Power Spectrum Approximation	34
3.4.1 Optimal Power Spectrum Approximation Problem (FIR)	35
3.5 IIR-Based Power Spectrum Approximation	37
3.5.1 Optimal Power Spectrum Approximation Problem (IIR)	37
3.6 Frequency Selection Algorithm	40
4 Examples	3
4.1 Summary	43
4.2 FIR Filter Design	43
4.2.1 Example 1	43
4.2.2 Example 2	50
4.3 IIR Filter Design	55
4.3.1 Example 3	5
4.3.2 Example 4	66
4.4 Power Spectrum Estimation	72
4.4.1 Example 5	72
4.4.2 Example 6	77
4.5 Model Reduction	83
4.5.1 Example 7	83
5 CONCLUSION	87
5.1 Conclusions	87
5.2 Contributions	89
5.3 Future Work	90
BIBLIOGRAPHY	91

LIST OF FIGURES

1	Ideal Low Pass Filter, Magnitude Frequency Characteristics For Example 1	45
2	Ideal Low Pass Filter, Phase Frequency Characteristics For Example 1	45
3	Remez Vs LMI-Based, No Weight For T. Band, Example 1	47
4	Remez Vs LMI-Based, 0.1 Weight For T. Band, Example 1	47
5	Remez Vs LMI-Based, 0.0001 Weight For T. Band, Example 1	47
6	Remez Error Over the Pass/Stop Bands	48
7	LMI-Based Error, No Weight	48
8	LMI-Based Error, 0.1 Weight	48
9	LMI-Based Error, 0.0001 Weight	49
10	Remez vs LMI-Based Phase Error	49
11	Ideal High Pass Filter, Frequency Mag. Characteristics for Example 2	51
12	Ideal High Pass Filter, Phase Frequency Characteristics for Example 2	51
13	Remez vs LMI-Based with Frequency Selection	53
14	Remez vs LMI-Based with Frequency Selection, Phase	53
15	Frequency Selection Error vs Normal LMI-Based with 56 Points	54
16	Frequency Selection Error vs Normal LMI-Based with 300 Points	54
17	Ideal Low Pass Filter, Mag. Frequency Characteristics for Example 3	56
18	Ideal Low Pass Filter, Phase Frequency Characteristics for Example 3	56
19	Ideal vs LMI-Based, with Weight for T.B., Unstable, Example 3	60
20	Ideal vs LMI-Based Phase, with Weight for T.B., Unstable, Example 3	60
21	LMI-Based, with Weight, Unstable, Error for the Pass/Stop Bands	61
22	Ideal vs the Stabilized LMI-Based	61
23	Ideal Phase vs the Stabilized LMI-Based Phase	61
24	Error Between Ideal and Stabilized LMI-Based Filters	62

25. Ideal vs LMI-Based (Stable), with No Weight, Example 3	62
26. Ideal Phase vs LMI-Based (Stable), with No Weight, Example 3	62
27. LMI-Based (Stable) Error Over All Bands	63
28. Ideal vs Yule Walker, Example 3	63
29. Ideal Phase vs Yule Walker Phase, Example 3	63
30. Yule Walker Error Over all Bands	64
31. Ideal vs Elliptic, Example 3	64
32. Ideal Phase vs Elliptic Phase, Example 3	64
33. Elliptic Filter Error for the Pass & Stop Bands	65
34. Elliptic Filter Magnitude Error over the Pass & Stop Bands	65
35. Ideal High Pass Filter, Frequency Mag. Characteristics for Example 4	67
36. Ideal High Pass Filter, Phase Frequency Characteristics for Example 4	67
37. Ideal vs LMI-Based with Frequency Selection	69
38. Error Between Ideal and LMI-Based with Freq. Selection	70
39. LMI-Based with no Freq. Selection $L=38$ vs Ideal	70
40. Error Between LMI-Based with no Freq. Selection and Ideal	70
41. LMI-Based with no Freq. Selection $L=300$ vs Ideal	71
42. Error Between LMI-Based with no Freq. Selection $L=300$ and Ideal	71
43. Power Spectrum Characteristics for Example 5	73
44. LMI-Based Approximation with $N=20$	75
45. LMI-Based Approximation Error with $N=20$	75
46. LMI-Based Approximation with $N=16$	75
47. LMI-Based Approximation Error with $N=16$	76
48. LMI-Based Approximation with $N=12$	76
49. LMI-Based Approximation Error with $N=12$	76
50. Power Spectrum Characteristics for Example 6	78
51. LMI-Based Approximation with $N=14$	81
52. LMI-Based Approximation Error with $N=14$	81
53. LMI-Based Approximation with $N=10$	81

54. LMI-Based Approximation Error with $N=10$	82
55. LMI-Based Approximation with $N=8$	82
56. LMI-Based Approximation Error with $N=8$	82
57. Desired Frequency Characteristics	84
58. Desired Frequency Characteristics, Phase	84
59. The Desired vs the Approximation	86
60. The Equiripple Error Behavior	86

LIST OF TABLES

1. Weight Effect on Approximation Error, Example 1, FIR Case	45
2. Number of Frequency Points Effect on Error, Example 1, FIR Case	53
3. Weight and Stabilization Effect on Approximation Error, Example 3, IIR	60
4. No. of Frequency Points Effect on T. & P/S Bands Errors, Example 4	69
5. Algorithm Sensitivity to Initial $d(.)$	69
6. The Effect of the Approximation Order on Error	74
7. The Effect of the Approximation Order on Error	78
8. Model Reduction Approximation Results	86

ABSTRACT

Name: Wasim Mohamed Munther Al-Baroudi
Title: Digital Filter Design Using LMI Based Techniques
Major Field: Systems Engineering
Date of Degree: June 1997

Linear Matrix Inequalities (LMI) based digital filter design algorithms are developed and applied to the FIR (one dimensional) optimal filter design problem and FIR (one dimensional) power spectrum estimation problem. The IIR (one dimensional) LMI based digital filter design and IIR (one dimensional) power spectrum estimation problems are formulated as linear objective optimization problems with LMI constraints and solved using an alternative scheme to overcome the non-linearity optimization formulation. In addition, the LMI based formulation of the filter design problem is applied to general approximation/model reduction problems (SISO). The solutions obtained by solving several examples show better results as compared with the traditional design methods.

Master of Science Degree
King Fahd University of Petroleum and Minerals
Dhahran, Saudi Arabia
June, 1997

خلاصة الرسالة

اسم الطالب : وسيم محمد منذر البارودي.
 عنوان الرسالة : تصميم الفلاتر الرقمية باستخدام تقنية المصفوفات الخطية الغير متساوية.
 التخصص : هندسة النظم والأساليب .
 تاريخ التخرج : صفر ١٤١٨.

لقد تم تطوير طريقة لتصميم الفلاتر الرقمية باستخدام تقنية المصفوفات الخطية الغير متساوية و تم تطبيق هذه الطريقة على مسألة تصميم الفلاتر أحادية الاتجاه المثلى التي لها استجابة نبضية محدودة (FIR) ولها استجابة نبضية غير محدودة (IIR). و باستخدام تقنية المصفوفات الخطية الغير متساوية نفسها تم أيضا تكوين و حل مسألة التقريب الأمثل لدالة طيف الطاقة لنماذج لها استجابة نبضية محدودة (FIR) ولها استجابة نبضية غير محدودة (IIR). و للتغلب على المشكلة اللاحقة في تكوين المسائل المتعلقة بالفلاتر التي لها استجابة نبضية غير محدودة (IIR) تم تطوير طريقة دورية تقريبية تعتمد على تثبيت قيمة المقام أثناء حل المسألة في كل دورة ثم نقل القيمة المثلى إلى الدورة التالية. و كتأكيد على القدرة التطبيقية للطريقة تم تطبيق تقنية المصفوفات الخطية الغير متساوية على مسألة تقريب النماذج أحادية الداخل و الخارج (SISO). النتائج المستخرجة من الأمثلة المحولة جيدة بالمقارنة ببعض الطرق التقليدية.

درجة الماجستير في العلوم
 جامعة الملك فهد للبترول و المعادن
 الظهران - المملكة العربية السعودية

صفر ١٤١٨

CHAPTER 1

INTRODUCTION

1.1 Literature Survey

Filter design is one of the most important problems in Signal Processing. Many techniques are available to design analog as well as digital filters. However, research in the area of digital filter design is still active to find new kinds of filters with better performance and the methods for designing them, or to provide more reliable, efficient and convenient design algorithms. The procedure for designing digital filters usually has four steps [1]:

1. Form of specifications for a digital filter.
2. Synthesis of the filter transfer function $H(z^{-1})$.
3. Realization of $H(z^{-1})$.
4. Simulation.

In general, filters are divided into two main categories according to the length of their impulse response:

- Recursive or IIR filters
- Nonrecursive or FIR filters

IIR filters can approximate a given ideal filter with lower order than FIR filters. This introduced the practice of applying order reduction techniques after designing FIR filters [2]. FIR filters can have linear phase while IIR filters have nonlinear phase. The problem of stability does not exist for FIR filters, while for IIR filters one has to make sure that the resulting filter is stable [3]. Linear phase digital filters are of special interest among the mixed phase digital filters. Despite distortion of magnitude response, if a digital filter has a linear phase property, the output of the filter can keep odd and even symmetric properties of the input signal [1]. However, Linear phase is not required for the stopbands since the rejected signal is not of interest.

There are several techniques available for FIR and IIR filter design [3]. Optimal FIR filters techniques started in the 1970's. Mainly Remez Exchange Algorithm was the basis of these techniques, which was inherently built for SISO filters. The algorithm proposed by Parks and McClellan uses the Remez exchange method to find the optimal approximation for the magnitude response. The formation of the design problem allows that the designed filters always have the exact specified band edges [1]. After that many algorithms were developed based on *Advanced Linear Programming Techniques*, *Quadratic Programming Techniques*, and *Lawson's Algorithm*. Focus of the new methods has been on better problem formulation to include new constraints, less computational efforts, speed of algorithm convergence, algorithm robustness, and the capability of handling complex coefficients filter [4].

In [4] and by using *Quadratic Programming*, better convergence rates were achieved due to the elimination of the linearization related steps. However, by using *Lawson's Algorithm* for solving repeated L_2 approximations and converging to the Chebychev solution, significant difficulties were introduced mainly due to the fact that the algorithm converged before reaching the correct solution. The reason was related to the vanishing weights changing each iteration [4]. To overcome this problem, Cortelazzo and Lightner applied a multiple criterion optimization technique to design both FIR and IIR digital filters. The method, however, could only be used for low order filters and requires considerable computing time [1]. Recent approaches, however, tackle this problem intelligently and introduce more efficient implementations to *Lawson's Algorithm* [4]. Tseng [4] enhanced *Lawson's Algorithm* performance by introducing a practical implementation that restarts the algorithm efficiently.

In general, methods based on using *Lawson's Algorithm* show a premature stopping problem handled sometime by heuristic methods that nobody proved its global convergence [4].

Recently, [5] introduced the use of Linear Matrix Inequalities (LMIs) to compute the FIR Chebychev approximation of a desired power spectrum or frequency response magnitude. It was shown that the constraints of the FIR Optimal Design Problem can be expressed as LMIs, and hence they can be easily handled by recent interior-point methods

In [4], an algorithm that best approximates, in the complex Chebychev sense, a desired complex valued frequency response was introduced. The algorithm is a variant of the simplex algorithm of linear programming. The algorithm used is robust and exhibits good

convergence speed to the global optimal solution and it can be used to design complex valued impulse response FIR filters.

The early IIR optimal design efforts started by developing least-squares approximation based methods to approximate only the filter magnitude response [1]. The errors of the designed filters were not equiripple. The least-squares based methods, in general, have difficulties in designing digital filters with sharp-cutoff transition bands, or with degrees higher than twelve [1].

Attempts to solve the minimax IIR design problem resulted in highly nonlinear optimization problems. In [6], an approach to solve the problem is given, however, the authors failed to obtain convergence to a global optimum and they were faced with a huge amount of computations. Approaches leading to the suboptimal Chebychev approximations mainly used linear and nonlinear programming [7-8], *Ellacott-Williams* algorithm based IIR design [9-10], and optimal Hankel norm filter design [11].

Recently, *Lawson's Algorithm* [13] was used to solve the weighted least-squares problem in IIR filter design [12], which may lead to unstable solutions and convergence is not guaranteed in some situations. Better versions with less computational efforts of this algorithm appeared more recently in [14-16].

In [17] a technique was introduced that can improve the performance of some IIR-based optimization algorithms [18]. The technique is based on the density of frequency samples. The author suggested the frequency samples set to be 3-6 times the number of variables. By doing this, spikes will disappear from the error function and the optimal error value will reduce significantly. The author, however, agreed that this would considerably increase the amount of computations required.

In [19] a way to best select the starting point of *Ellacott-Williams* algorithm was introduced. Previously, the starting point problem was addressed in [14] and solved partially by splitting the starting point selection into two steps so that only starting values for the poles are required. The numerator is found automatically by solving a linear approximation problem. The theoretical drawback of this modified *Ellacott-Williams* is that convergence to the local optimal approximation is not anymore guaranteed. This problem can be avoided by using a maximum likelihood estimator for the identification of the denominator transfer function [19].

A procedure to separate design of the numerator and the denominator was first investigated in 1972 [1]. First, an allpoles group delay filter is designed by using nonlinear optimization so that the error of the group delay in the passband is equiripple. Then a linear phase FIR filter is used to compensate the magnitude response so that an equiripple error is maintained.

Design of IIR filters with linear phase in the passband is receiving more focus due to order advantage over FIR filters [20-21]. One common approach is to design first an IIR filter that meets the magnitude specifications and then to use optimization methods to design all pass equalizer stages to correct the phase response. In [20], a technique based on model reduction of a FIR prototype using frequency weighting to improve the approximation in the transition region. Several model reduction techniques used in literature will lead to stable minimal realization IIR filter [22]. Another approach is to design IIR filters directly using optimization methods, mainly linear programming over a linearized model or heuristic methods, to meet both magnitude and phase characteristics simultaneously [22].

In [23], a method was presented to compute an optimal IIR filter that satisfies an arbitrary magnitude frequency response specified using a tolerance scheme. This method is suitable for the design of compensators, equalizers, and frequency-selective filters. It exhibits desirable convergence properties and numerical stability. A *modified Remez Algorithm* was used to solve the design problem.

In [22] new approaches have been proposed which depend on specifying a tolerance to magnitude frequency response to formulate the Chebychev norm objective function. This method will converge quadratically to the optimal solution of the tolerance problem with stable computation scheme using the multiple stage algorithms.

Rational approximations of high order transfer functions with lower order ones have important applications in Control Systems and Signal Processing applications. The L_∞ / H_∞ norm¹ is commonly used to measure the approximation error like in [24-28]. This is widely accepted and proved to be the most meaningful norm measure. This is mainly related to the fact that the H_∞ based optimization (Chebychev Norm) is a minimax operator that covers the whole range of frequency points to bring the maximum error between the ideal and the approximate functions to its minimum.

In [24] and [25], efficient algorithms were proposed to solve useful control optimization problems involving Linear Matrix Inequalities (LMI) constraints [24-25]. This is due to the fact that many control and signal processing problems can be formulated as *Linear Objective Optimization Problem* with LMIs constraints [29].

¹ $\|G\|_\infty = \max_{\omega \in [0, 2\pi)} |G(e^{j\omega})|$

During recent years, LMIs have attracted a lot of interest for solving H_∞ / L_∞ problems. Since model reduction problem can be considered a special case of L_∞ design with confined degree of controller, it seems natural to adopt LMIs for model reduction. However, formulation will yield a nonlinear problem where convergence is not guaranteed as in [30].

Specifically, the LMI based convex optimization approach was applied to approximation problems with L_∞ norm to measure the approximation error. In [24], [31] and [32], the approach was applied to the H_∞ norm model reduction problems.

In this thesis, several important signal processing and digital optimal filter design problems (both FIR and IIR) are formulated as *Linear Objective Optimization Problems* with LMI constraint. The algorithms are illustrated using many examples.

1.2 Scope of Work

The scope of this thesis is two-fold. First, LMI optimization technique will be applied to FIR optimal filter design problem and FIR power spectrum estimation problem. Second, the IIR filter design problem and the IIR power spectrum estimation problem will be considered.

1.2.1 L_∞ Optimal FIR Filter Design Problem

The research will focus on FIR optimal filter design by investigating several techniques of optimally approximating the desired characteristics filter using the L_∞ norm to minimize the error between the desired filter characteristics and the approximate filter. The resulting

problem is an L_∞ norm Approximation Problem that appears in many meaningful applications in Systems and Control theory.

Consider the desired discrete filter characteristic $G_d(j\omega)$ and an associated weight function $W(\omega)$. The problem is to find the optimal $G(j\omega) = n(j\omega) \in RL_\infty$ that solves

$$\begin{aligned} \min_{n(\cdot)} \quad & \gamma \\ \text{Subject to} \quad & \|W(\omega)(G_d(j\omega) - G(j\omega))\|_\infty < \gamma \quad \forall \omega \end{aligned}$$

1.2.2 L_∞ Optimal IIR Filter Design Problem

Techniques for optimally approximating the desired filter characteristics using the L_∞ norm error will be introduced.

Consider the desired discrete filter characteristic $G_d(j\omega)$ and an associated weight function $W(\omega)$. The problem is to find the optimal $G(j\omega) = \frac{n(j\omega)}{d(j\omega)} \in RL_\infty$ that solves

$$\begin{aligned} \min_{n(\cdot), d(\cdot)} \quad & \gamma \\ \text{Subject to} \quad & \|W(\omega)(G_d(j\omega) - G(j\omega))\|_\infty < \gamma \quad \forall \omega \end{aligned}$$

1.2.3 Optimal Power Spectrum Approximation Problem (IIR/FIR)

As a special formulation of the FIR and the IIR optimal filter design problems, the *Power Spectrum Approximation Problem* will also be solved using both FIR and IIR models. It will be assumed that the frequency response characteristics of the signal under estimation

are available by observing the signal $x(n)$, $-\infty < n < \infty$ for limited number of points. Then the FTT of the observed signal can be obtained using any of the *Classical Power Spectrum Estimation Techniques*. Usually, the *Classical Power Spectrum Estimation Techniques* will produce transfer functions with high orders to achieve acceptable estimate quality.

The *Power Spectrum Approximation Problem* will start by a frequency characteristics either given in the form of a transfer function or as a sequence $G_d(\omega_k) = G_k$, $k = 0, \dots, L$, $\omega_k \in [0, \pi]$. The problem is to maintain as much as possible the accuracy we get from applying the *Classical Power Spectrum Estimation Techniques* with less number of parameters.

Consider the discrete Power Spectrum characteristic $G_d(j\omega) = \hat{G}_d(j\omega)\hat{G}_d^*(j\omega) \geq 0$ and an associated weight function $W(\omega)$. The problem is to find the optimal $G(j\omega) = \hat{G}(j\omega)\hat{G}^*(j\omega)$ that solves

$$\begin{aligned} \min_{G(\cdot)} \quad & \gamma \\ \text{Subject to} \quad & \|W(\omega)(G_d(\omega) - G(j\omega))\|_{\infty} < \gamma \quad \forall \omega \end{aligned}$$

The problem of having large number of LMIs is valid for both the FIR and the IIR cases. We will apply the same approaches to reduce the number of frequency points needed to get acceptable results. Well-known examples from literature will be used to illustrate the results. Based on these examples, analysis will be conducted on the results to highlight the properties, advantages and disadvantages of the methods.

1.3 Organization

In Chapter 2, theoretical backgrounds and preliminaries will be introduced. In Chapter 3, the optimal L_∞ filter design algorithms will be derived and put in the form of the *Linear Objective Optimization Problem* with LMI constraint. Several examples illustrating the proposed algorithms will be given in Chapter 4 with an analysis of the results. Finally, the conclusions, contributions and future work for this thesis will be given in Chapter 5.

CHAPTER 2

PRELIMINARIES

2.1 Basics of LMI Based Optimization Techniques

In a recent book by Boyd [29], a full comprehensive treatment of LMI based convex optimization is given. In this book, many meaningful control and systems problems have been formulated as LMI problems.

A linear matrix inequality is given as

$$F(x) := F_0 + x_1 F_1 + \dots + x_m F_m \leq 0 \quad (1)$$

where the vector $x = (x_1, \dots, x_N) \in R^N$ is the *decision* or *optimization* vector and F_i 's are real symmetric matrices having all their eigen values in the left half plane. Clearly Inequality (1) is a convex constraint and any minimization problem having this constraint will be a linear convex optimization problem that will converge to the global optimum when solved. Inequality (1) is a set of N polynomial inequalities in x , where the leading principle minor $F(x)$ must be negative.

Multiple LMIs $F^{(1)}(x) < 0, \dots, F^{(p)} < 0$ can be expressed as the single LMI $\text{diag}(F^{(1)}, \dots, F^{(p)}(x)) < 0$. Hence, no distinction can be made between one LMI and multiple LMIs; they are solvable using the same methodology. In other words, multiple LMI constraints can be imposed on the decision vector x without destroying the problem convexity. When the matrices F_i 's are diagonal, the LMI $F(x) < 0$ is just a set of linear inequalities. The following very useful Lemma is used to convert some nonlinear convex inequalities into LMI.

Lemma 1 [29]

The linear matrix inequality given by

$$\begin{pmatrix} Q(x) & S(x) \\ S^T(x) & R(x) \end{pmatrix} \leq 0$$

where $Q(x) = Q^T(x)$, $R(x) = R^T(x) < 0$, and $S(x)$ depends affinely on x , is equivalent to having $Q(x) - S(x)R^{-1}(x)S^T(x) \leq 0$

Finding an x to satisfy the LMI system $F(x) < 0$ is called the *feasibility problem*, while minimizing a linear objective function under the LMI constraints is called the *linear objective minimization problem* and takes the form

$$\text{Min } c^T x \quad \text{subject to } F(x) < 0$$

The LMI formulation can be used to represent a wide variety of problems having convex constraints on x . In particular, linear inequalities, convex quadratic inequalities, matrix norm inequalities, and constraints that arise in control theory, such as Lyapunov and convex quadratic matrix inequalities, can all be cast in the form of an LMI. Further

applications of LMIs arise in H_∞ control, estimation, identification, and optimal design [34].

Efficient interior point algorithms are now available to solve the feasibility and the linear objective minimization LMI problems. These algorithms have a polynomial-time complexity. That is, the number $N(\varepsilon)$ of flops needed to compute an ε -accurate solution is bounded by $N(\varepsilon) \leq M N^3 \log(V / \varepsilon)$, where M is the total row size of the LMI system, N is the total number of scalar decision variables, and V is a data-dependent scaling factor. In this thesis, the LMI Lab MATLAB[®] toolbox will be used for implementing the algorithms solving the LMI based problems.

2.2 Filter Design Techniques

FIR filters have the input-output relationship.

$$y(n) = b_0 x(n) + b_1 x(n-1) + \dots + b_N x(n-N) = \sum_{k=0}^N b_k x(n-k)$$

This characterizes FIR filter response of order N . Note that the output depends only on the input. Moreover, causality is assumed since k appears only with a positive value or 0. FIR filters are characterized in the complex frequency domain by the following transfer function.

$$H(z) = \sum_{k=0}^N b_k z^{-k}$$

The IIR filter has the following input-output relationship.

$$y(n) = a_1 y(n-1) + a_2 y(n-2) + \dots + a_M y(n-M) + b_0 x(n) + b_1 x(n-1) + \dots + b_N x(n-N)$$

$$y(n) = \sum_{k=0}^N b_k x(n-k) + \sum_{k=1}^M a_k y(n-k)$$

This characterizes an IIR filter response. Note that the output depends on the input and the output. Moreover, causality is assumed since k assumes only non-negative values. The IIR filter is characterized in the complex domain by the following transfer function.

$$H(z) = \frac{\sum_{k=0}^N b_k z^{-k}}{\sum_{k=1}^N a_k z^{-k}}$$

2.2.1 Filter Design Problem

The desired filter characteristics are usually specified in the frequency domain in terms of desired magnitude and phase responses. The filter design technique is used, then, to find the coefficients of a causal FIR or IIR filter (b_i 's & a_i 's) closely approximating the desired frequency response specifications.

It is the designer choice to use IIR or FIR filter to meet his design requirements. It all depends on the specific requirements expected from the designed filter. Usually FIR filters are employed in problems where linear phase over the passband is needed. Otherwise both IIR and FIR are used. As a general rule, IIR filters have lower sidelobes in the stopband than FIR filters having the same number of parameters. In cases where phase response is either unimportant or distortion is tolerable, IIR will have much fewer parameters, less memory requirements, and lower computational complexity during the design process.

2.2.2 FIR Filter Design

Windowing is a well-known technique for designing FIR filters where it starts by defining the desired frequency response $H_d(\omega)$ and a window in the frequency domain $W(\omega)$ having linear phase characteristics. There exist several types of windowing techniques (Rectangular, Hamming, Hanning, Blackman, ...) each of which has its own case-based usage.

Frequency-Sampling technique is another FIR design technique where it starts also by defining the desired frequency response $H_d(\omega)$ as a set of equally spaced frequencies, namely

$$\begin{aligned}\omega_k &= \frac{2\pi}{M}(k + \alpha) & , \quad k = 0, 1, \dots, \frac{M-1}{2}, \quad M \text{ odd} \\ & & k = 0, 1, \dots, \frac{M}{2} - 1, \quad M \text{ even} \\ \alpha &= 0 \text{ or } \frac{1}{2}\end{aligned}$$

The designed filter is obtained by solving the unit sample response of the FIR filter from these equally spaced frequency specifications. Sometimes, linear programming techniques are used to optimize the transition band frequency specifications.

The *Chebyshev norm approximation* (L_∞ Norm Approximation) is also used to design a filter that minimizes the maximum approximation error between the desired and the actual frequency responses. The weighted approximation error may be expressed as

$$E(\omega) = W(\omega)[H_d(\omega) - P(\omega)]$$

where $P(\omega)$ is the actual frequency response of the filter $\alpha(k)$. Then the problem will be

$$\min_{\text{over } \alpha(k)} [\max_{\omega \in S} |E(\omega)|] \quad (2)$$

where S represents the set of frequency band over which the optimization is to be performed. Basically, the set S consists of the passbands and the stopbands frequencies of the desired filter. The solution to this problem was introduced in 1972 by Parks and McClellan [35] and they introduced the alternative theorem for Chebychev approximation theory. The *Chebychev norm approximation* (L_∞ Norm Approximation) is the problem of concern for this thesis. Basically, the *Optimal Filter Design Problem*, the *Optimal Power Spectrum Approximation Problem*, and the *Model Reduction Problem* can be formulated as a *Chebychev norm approximation problem with LMI constraints*. Then, an LMI-Based algorithm will be developed to solve the *Chebychev norm approximation problem*.

Alternation Theorem: [35] *Let S be a compact subset of interval $[0, \pi)$. A necessary and sufficient condition for $P(\omega)$ to be the unique, best weighted Chebychev approximation to $H_d(\omega)$ in S is that the error function $E(\omega)$ exhibit at least $L+2$ external frequencies in S . That is, there must exist at least $L+2$ frequencies $\{\omega_i\}$ in S such that $\omega_1 < \omega_2 < \dots < \omega_{L+2}$, $E(\omega_i) = -E(\omega_{i+1})$ and*

$$|E(\omega_i)| = \max_{\omega \in S} |E(\omega)|, \quad i = 1, 2, \dots, L+2. \quad (L \text{ is the filter order})$$

In simple words, the above theorem means that when the optimal (*Global*) filter coefficients $\alpha(k)$ are achieved for the problem in Equation (2), the error function $E(\omega)$ alternates in sign between two successive external frequencies. *Remez exchange algorithm* is practically used to compute the optimal solution of Equation (2) [35]. This starts by guessing the set of external frequencies, and then computing the error function $E(\omega)$.

Then the algorithm will iterate to find the optimal set of external points. The algorithm will stop when $|E(w)| \leq \delta$ for all frequencies in the dense set S ; practically selected to be at least $16M$, where M is the order of the estimated FIR filter. *Remez exchange algorithm* has more recent algorithms with better computational advantages [35].

In general, the minimax optimal approximation methods for designing filters has the advantage of providing total optimal control of the filter specifications and, as a consequence, it is usually preferable over all non-optimal methods like the *Windowing* method and the *frequency sampling* method.

2.2.3 IIR Filter Design

Since analog IIR filter design is a mature and well developed field, early digital filter design techniques started with designing the filter in the analog domain and then converting it into the digital domain. Several effective conversion techniques can be used under the following conditions:

- The $j\omega$ axis in the s-plane map into the unit circle in the z-plane.
- The left-half plane of the s-plane map into the inside of the unit circle in the z-plane.

The first condition will guarantee that frequencies are mapped with one-to-one relationship and the second condition will maintain stability of the filter after the conversion. It is a well-known fact that a stable, causal IIR filter cannot have linear phase [35].

One of the most widely used conversion methods is the bilinear transformation, where s is replaced by:

$$s = \frac{2(1 - z^{-1})}{T(1 + z^{-1})}.$$

Some of the commonly used analog filter characteristics are:

Butterworth Filters: Butterworth all-poles filters have the property that they are maximally flat. Their frequency characteristic is determined by

$$\|H(\omega)\|^2 = \frac{1}{1 + (\omega / \omega_c)^{2N}} = \frac{1}{1 + \varepsilon^2 (\omega / \omega_p)^{2N}}$$

Where N is the filter order, $1/(1+\varepsilon^2)$ is the band-edge value and ω_c is its cutoff frequency. ω_p is the passband edge frequency. The Butterworth filter is completely determined by the parameter N , δ_2 (attenuation at a specified ω_s), ε and the ratio ω_s/ω_p .

Chebyshev Filters: Type I filters are all pole filters that have equiripple behavior in the passband and monotonic behavior in the stopband. Type II Chebyshev filters contain both poles and zeros and they have monotonic behavior in passband and equiripple behavior in the stopband. The Type I filter magnitude is given as

$$\|H(\omega)\|^2 = \frac{1}{1 + \varepsilon^2 \tau_N^2(\omega / \omega_p)}$$

where ε is a parameter of the filter related to the ripple in the passband and τ_N is the N th order Chebyshev polynomial. Type II Chebyshev filter has the characteristic

$$\|H(\omega)\|^2 = \frac{1}{1 + \varepsilon^2 \left[\tau_N^2(\omega_s / \omega_p) / \tau_N^2(\omega_s / \omega) \right]}$$

ω_p is the passband frequency and ω_s is the stopband frequency.

Elliptic Filters: Elliptic filters have the smallest order in comparison with the Butterworth and Chebyshev filters but its phase characteristics are highly nonlinear. The

phase characteristics of elliptic filters are more nonlinear in the passband in comparison with the former ones. The characteristic of the Elliptic filters are given by:

$$|H(\omega)|^2 = \frac{1}{1 + \varepsilon^2 U_N(\omega / \omega_p)}$$

where $U_N(x)$ is the Jacobian elliptic function of order N , and ε is a parameter related to the passband ripples.

There are several digital IIR filter design techniques available that optimally approximates the desired filter response by an IIR filter. Some of these techniques will require the desired response to be in the time domain, like the *Pade Approximation Technique*, *Least Squares Design Method* and other techniques requires it to be in the frequency domain. However, both methods will design a digital filter directly without any conversion.

The Least Square Design Method can be used to design IIR filters in the frequency domain. Assume that the IIR filter is given by:

$$H(z) = GA(Z) = G \prod_{k=1}^K \frac{1 + \beta_{k1}z^{-1} + \beta_{k2}z^{-2}}{1 + \alpha_{k1}z^{-1} + \alpha_{k2}z^{-2}},$$

where G is the filter gain and the set of coefficients $\{\alpha_{k1}\}$, $\{\alpha_{k2}\}$, $\{\beta_{k1}\}$, $\{\beta_{k2}\}$ are to be determined. Also assume that the frequency response is given by

$$H(\omega) = GA(\omega)e^{j\Theta(\omega)},$$

where $\Theta(\omega)$ is the phase response. Let $A_d(\omega)$ be the desired magnitude frequency response over arbitrary spaced frequencies ω_k , $k=1,L$. Then the error in magnitude function at ω_k 's is $GA(\omega_k) - A_d(\omega_k)$ and the least square objective function would be:

$$\xi(p, G) = \sum_{n=1}^L w_n [GA(\omega_n) - A_d(\omega_n)]^2 \quad (3)$$

where p denotes a 4K-dimensional vector of filter coefficients $\{\alpha_{k1}\}$, $\{\alpha_{k2}\}$, $\{\beta_{k1}\}$, $\{\beta_{k2}\}$, and $\{\omega_n\}$ is weighting factor. Another version of Equation (3) exists where the error in phase between the ideal specifications and the actual approximation is added. This can be used when the phase behavior is of importance to the designer.

Obviously, the problem is having a nonlinear objective function in Equation (3). This can be solved using iterative numerical optimization methods such as the Fletcher and Powell method (1963) [35], linear and nonlinear programming [7-8], *Ellacott-Williams* algorithm based IIR design [9-10], and optimal Hankel norm filter design [11]. The solution, however, is not guaranteed to converge to a global optimum.

2.3 Power Spectrum Estimation

The basic problem that comes in power spectrum estimation is the estimation of power density spectrum of a signal observed over a finite time interval. Actually, the finite length of the data sequence is a major limitation on the quality of the estimate. If the signal statistics are stationary, the more points taken, the better quality the estimate will be.

The signal under estimation can be either deterministic or random. For deterministic, stationary signal, let $x(n)$, $-\infty < n < \infty$ be the sample response of the sequence under estimation. This has a Fourier transform (Voltage spectrum) of

$$X(\omega) = \sum_{n=-\infty}^{\infty} x(n)e^{-j\omega n} \quad \text{or} \quad X(f) = \sum_{n=-\infty}^{\infty} x(n)e^{-j2\pi f n}$$

where $f = F / F_s$ is the normalized frequency variable. Consequently, the energy density spectrum of the sampled signal is $S_{xx}(\omega) = |X(\omega)|^2$. It is good to note that $S_{xx}(\omega)$ can also be obtained also by taking the Fourier transform of the autocorrelation function of the signal $x(n)$, $-\infty < n < \infty$ [35].

There exist two approaches of dealing with the power spectrum estimation. First, assume nothing about how the data $x(n)$, $-\infty < n < \infty$ was generated, usually called *nonparametric methods*. Estimates following these methods will result at the best with a frequency resolution equal to the spectral of a rectangular window of length N . This is mainly caused by the finite length of data used. The *nonparametric methods* mainly depend on decreasing the frequency resolution for reducing variance in the spectral estimate. The main drawback with the *nonparametric* methods is the need for large data in order to yield the necessary frequency resolution required in many applications [35].

The second approach depends on the assumption that we have some a priori information on how the data was generated. In such a case a model for the signal generation may be constructed with a number of parameters that can be estimated from the observed data. Then, from the model and the estimated parameters, we can compute the power density spectrum implied by the model. This approach is usually called the *parametric (model-based)* power spectrum estimation methods. These methods will provide better frequency resolution than the *nonparametric* ones, especially when little data is available.

The model assumed by the parametric methods is usually characterized by a rational linear system function of the form

$$H(z) = \frac{B(z)}{A(z)} = \frac{\sum_{i=1}^N b_i z^{-i}}{1 + \sum_{l=1}^M a_l z^{-l}}.$$

2.4 Characterization of the Solution for L_∞ Norm

Approximation

Least squares rational approximation was the main tool of approximation because there were no other tractable solutions. Important breakthrough results on Hankel norm related approximation emerged in early 80s [32]. Lately, the L_∞ norm approximation problem itself has found many meaningful applications in Systems and Control theory. In the frequency domain, $\|G\|_\infty = \sup_{\omega} |G(j\omega)|$, which means the distance in the complex plane from the origin to the farthest point in the Nyquist plot.

2.4.1 L_∞ Approximation Problem (SISO Systems)

Given a transfer function $G(z) \in RL_\infty$ with degree n , find the optimal transfer function

$G_r(z) = \frac{n(z)}{d(z)} \in RL_\infty$ with degree $r < n$, such that $\|W(G - G_r)\|_\infty$ is minimized, where W is

the weight, and $\|G\|_\infty := \sup_{\omega} |G(e^{j\omega})|$.

$$\begin{aligned} \min_{n(z), d(z)} \quad & \alpha \\ \text{S.T.} \quad & \|W(G - G_r)\|_\infty < \alpha \end{aligned}$$

where L_∞ is the space of functions of a complex variable that are bounded on the $j\omega$ -axis (bounded but possibly not stable) and H_∞ is the space of functions of a complex variable

that are analytic in the right half plane (stable). An alternative way of stating the L_∞ norm approximation problem is as follows [36]: *Find the best $G_r(z)$ so that the error function $E(e^{j\omega}) = G(e^{j\omega}) - G_r(e^{j\omega})$ is contained inside a disc around 0, having minimal radius.*

If $E(e^{j\omega}) = 1$, the error curve is said to be circular. A priori not much is known about the problem except that the error curve should be enclosed inside a circle with minimum radius and it must touch the circle on at least $r + 2$ points, where r is the order of the approximation. Experience shows that for most cases, the optimal error curve has winding number $2r + 1$ and is near circular [28]. The following theorem relates near circularity to near optimality [36].

Theorem 1 [28]

Suppose the error curve for a $G_r(z)$ has winding number at least $2r + 1$ about the unit origin. Then

$$\min_{\omega} |G(e^{j\omega}) - G_r(e^{j\omega})| \leq |G^*(e^{j\omega}) - G_r^*(e^{j\omega})| \leq \|G - G_r\|_\infty$$

where $G_r^(z)$ is an optimal approximant.*

An immediate corollary of this theorem is that if for such $G_r(z)$ the upper and lower bounds are equal, i.e., the error is perfectly circular, then $G_r(z)$ is optimal [28].

CHAPTER 3

LMI BASED FILTER DESIGN

3.1 L_∞ Optimal Filter Design Problem

Considering the criteria of measuring the error between the desired characteristics and the optimal approximation to be the L_∞ norm, the main problem of this section will be as follows.

3.1.1 The Problem

Consider the ideal discrete filter characteristic $G_d(j\omega)$ and an associated weight function

$\Delta \omega$. The problem is to find the optimal $G(j\omega) = \frac{n(j\omega)}{d(j\omega)} \in RL_\infty$ that solves

$$\begin{aligned} \min_{n(\cdot), d(\cdot)} \quad & \gamma \\ \text{Subject to} \quad & \|W(\omega)(G_d(j\omega) - G(j\omega))\|_\infty < \gamma \quad \forall \omega \end{aligned} \quad (4)$$

The constraint in Equation (4) is not an LMI, however, it can be brought into LMI format after applying one of following two approaches.

Approach 1

$$\|W(\omega)(G_d(j\omega) - G(j\omega))\|_\infty < \gamma, \quad \forall \omega \Leftrightarrow$$

$$W(\omega)(G_d(j\omega) - G(j\omega))(G_d(j\omega) - G(j\omega))^* W^*(\omega) < \gamma^2, \quad \forall \omega \Leftrightarrow$$

$$W(\omega)(G_d(j\omega) - \frac{n(j\omega)}{d(j\omega)})(G_d(j\omega) - \frac{n(j\omega)}{d(j\omega)})^* W^*(\omega) < \gamma^2, \quad \forall \omega$$

By multiplying both inequality sides by $d(j\omega)d^*(j\omega) > 0$, the inequality will become

$$W(\omega)W^*(\omega)[d(j\omega)G_d(j\omega) - n(j\omega)][d(j\omega)G_d(j\omega) - n(j\omega)]^* < \gamma^2 d(j\omega)d^*(j\omega), \quad \forall \omega \Leftrightarrow$$

$$-\gamma^2 d(j\omega)d^*(j\omega) + W(\omega)W^*(\omega)[d(j\omega)G_d(j\omega) - n(j\omega)][d(j\omega)G_d(j\omega) - n(j\omega)]^* < 0, \quad \forall \omega$$

By applying Lemma 1, we get

$$\begin{pmatrix} -\alpha d(j\omega)d^*(j\omega) & W(\omega)^*[d(j\omega)G_d(j\omega) - n(j\omega)]^* \\ W(\omega)[d(j\omega)G_d(j\omega) - n(j\omega)] & -1 \end{pmatrix} < 0, \quad \forall \omega \quad (5)$$

where $\gamma = \sqrt{\alpha}$.

Hence, Equation (4) will become

$$\min_{n(\cdot)d(\cdot)} \alpha$$

$$S.T. \begin{pmatrix} -\alpha d(j\omega)d^*(j\omega) & W(\omega)^*[d(j\omega)G_d(j\omega) - n(j\omega)]^* \\ W(\omega)[d(j\omega)G_d(j\omega) - n(j\omega)] & -1 \end{pmatrix} < 0, \quad \forall \omega \quad (6)$$

Assuming that the approximate filter has real coefficients, then $\omega \in [0, \pi]$ is the frequency range needed to approximate the ideal filter characteristics. Notice that Equation (5) has to be satisfied in infinitely many frequencies in $[0, \pi]$ in order to solve

Equation (6). An approximate way of implementing Equation (6) is to discretize $\omega_i = i\Delta\omega$ for small enough $\Delta\omega$. This leads to the following optimization problem

$$\begin{aligned} & \min_{n(\cdot), d(\cdot)} \alpha \\ & S.T. \quad \begin{pmatrix} -\alpha d(j\omega_i) d^*(j\omega_i) & W(\omega_i)^* [d(j\omega_i) G_d(j\omega_i) - n(j\omega_i)]^* \\ W(\omega_i) [d(j\omega_i) G_d(j\omega_i) - n(j\omega_i)] & -1 \end{pmatrix} < 0 \quad (7) \\ & \text{for } \omega_i = i\Delta\omega, \quad i = 0, \dots, L, \quad \Delta\omega = \pi / L. \end{aligned}$$

In the FIR design case, where $d(j\omega) = 1$, Equation (7) would be a proper *Linear Objective Minimization Problem (LOMP)* having an LMI constraint. However, in the IIR case, it will not have an LMI constraint because of the term $-\alpha d(j\omega) d^*(j\omega)$.

Approach 2

$$\|W(\omega)(G_d(j\omega) - G(j\omega))\|_\infty < \gamma, \quad \forall \omega \Leftrightarrow$$

$$W(\omega)(G_d(j\omega) - G(j\omega))(G_d(j\omega) - G(j\omega))^* W^*(\omega) < \gamma^2, \quad \forall \omega \Leftrightarrow$$

$$W(\omega)(G_d(j\omega) - \frac{n(j\omega)}{d(j\omega)})(G_d(j\omega) - \frac{n(j\omega)}{d(j\omega)})^* W^*(\omega) < \gamma^2, \quad \forall \omega$$

By multiplying both inequality sides by $d(j\omega) d^*(j\omega) > 0$, it becomes

$$\begin{aligned} & W(\omega) W^*(\omega) [d(j\omega) G_d(j\omega) - n(j\omega)] [d(j\omega) G_d(j\omega) - n(j\omega)]^* < \gamma^2 d(j\omega) d^*(j\omega), \quad \forall \omega \Leftrightarrow \\ & -\gamma^2 d(j\omega) d^*(j\omega) + W(\omega) W^*(\omega) [d(j\omega) G_d(j\omega) - n(j\omega)] [d(j\omega) G_d(j\omega) - n(j\omega)]^* < 0, \quad \forall \omega \end{aligned}$$

Let $A(j\omega) = d(j\omega) G_d(j\omega)$, where $d(j\omega)$ appears linearly. Then,

$$-\gamma^2 d(j\omega) d^*(j\omega) + W(\omega) W^*(\omega) [A(j\omega) - n(j\omega)] [A(j\omega) - n(j\omega)]^* < 0, \quad \forall \omega \Leftrightarrow$$

$$-\gamma^2 d(j\omega) d^*(j\omega) + W(\omega) W^*(\omega) [(A_r(\omega) - n_r(\omega))^2 + (A_i(\omega) - n_i(\omega))^2] < 0, \quad \forall \omega \Leftrightarrow$$

Where $A_r(\omega) = \text{Re}(A(j\omega))$, and $A_i(\omega) = \text{Im}(A(j\omega))$, and similarly, $n_r(\omega) = \text{Re}(n(j\omega))$, and $n_i(\omega) = \text{Im}(n(j\omega))$.

$$-\gamma^2 d(j\omega)d^*(j\omega) + W(\omega)W^*(\omega) \begin{pmatrix} A_r(\omega) - n_r(\omega) & A_i(\omega) - n_i(\omega) \end{pmatrix} \begin{pmatrix} A_r(\omega) - n_r(\omega) \\ A_i(\omega) - n_i(\omega) \end{pmatrix} < 0, \forall \omega$$

By applying Lemma 1, we get

$$\begin{pmatrix} -\alpha d(j\omega)d^*(j\omega) & W^*(\omega)(A_r(\omega) - n_r(\omega)) & W^*(\omega)(A_i(\omega) - n_i(\omega)) \\ W(\omega)(A_r(\omega) - n_r(\omega)) & -1 & 0 \\ W(\omega)(A_i(\omega) - n_i(\omega)) & 0 & -1 \end{pmatrix} < 0, \forall \omega \quad (8)$$

where $\gamma = \sqrt{\alpha}$.

Assuming that the approximate filter has real coefficients, then $\omega \in [0, \pi]$ is the frequency range needed to approximate the ideal filter characteristics. Notice that Equation (8) has to be satisfied in infinitely many frequencies in $[0, \pi]$ to reach the optimal solution. An approximate way of implementing Equation (6) is to discretize $\omega_i = i\Delta\omega$ for small enough $\Delta\omega$. This leads to the following optimization problem

$$\begin{aligned} & \min_{n(\cdot), d(\cdot)} \alpha \\ & \text{S.T.} \begin{pmatrix} -\alpha d(j\omega_i)d^*(j\omega_i) & W^*(\omega_i)(A_r(\omega_i) - n_r(\omega_i)) & W^*(\omega_i)(A_i(\omega_i) - n_i(\omega_i)) \\ W(\omega_i)(A_r(\omega_i) - n_r(\omega_i)) & -1 & 0 \\ W(\omega_i)(A_i(\omega_i) - n_i(\omega_i)) & 0 & -1 \end{pmatrix} < 0, \quad (9) \\ & \text{for } \omega_i = i\Delta\omega, \quad i = 0, \dots, L, \quad \Delta\omega = \pi / L \end{aligned}$$

Like *approach 1*, In the FIR design case, since $d(j\omega) = 1$, Equation (9) would have an LMI constraint. However, in the IIR case, the constraint is not an LMI because of the term $-\alpha d(j\omega)d^*(j\omega)$.

3.2 The FIR Case

Consider the case $d(z) = 1$ and $n(z) = b_0 + b_1 z^{-1} + \dots + b_N z^{-N}$, where N is the FIR filter order. In this case Equation (7) from *approach 1* reduces to the following LOMP.

$$\begin{aligned} \min_{\alpha} \alpha \\ S.T. \quad & \begin{pmatrix} -\alpha & W(\omega_i)^* [G_d(j\omega_i) - n(j\omega_i)]^* \\ W(\omega_i) [G_d(j\omega_i) - n(j\omega_i)] & -1 \end{pmatrix} < 0 \\ \text{for } & \omega_i = i\Delta\omega, \quad i = 0, \dots, L, \quad \Delta\omega = \pi / L. \end{aligned} \quad (10)$$

which is a complex LMI as a constraint. In order to convert this constraint to a real LMI we do the following. Consider (letting $z = e^{j\omega}$)

$$\begin{aligned} n(e^{j\omega}) &= b_0 + b_1(\cos \omega - j \sin \omega) + b_2(\cos 2\omega - j \sin 2\omega) + \dots + b_N(\cos N\omega - j \sin N\omega) \\ &= (b_0 + b_1 \cos \omega + b_2 \cos 2\omega + \dots + b_N \cos N\omega) - j(b_1 \sin \omega + b_2 \sin 2\omega + \dots + b_N \sin N\omega) \end{aligned}$$

Then,

$$\text{Re}(n(e^{j\omega})) = n_r(\omega) = \begin{pmatrix} b_0 & b_1 & \dots & b_N \end{pmatrix} \begin{pmatrix} 1 \\ \cos \omega \\ \vdots \\ \cos N\omega \end{pmatrix} = \bar{b} \bar{C}_N(\omega)$$

$$\text{Im}(n(e^{j\omega})) = n_i(\omega) = \begin{pmatrix} b_0 & b_1 & \cdots & b_N \end{pmatrix} \begin{pmatrix} 0 \\ \sin \omega \\ \vdots \\ \sin N\omega \end{pmatrix} = \bar{b} \bar{S}_N(\omega)$$

$$n(e^{j\omega}) = \bar{b} \bar{C}_N(\omega) - j \bar{b} \bar{S}_N(\omega) \quad (11)$$

Consider an ideal linear phase filter characteristic to be

$$G_d(j\omega) = |G_d(j\omega)| e^{-j\frac{N}{2}\omega} = G_{dr}(\omega) + jG_{di}(\omega)$$

where N is the order of the approximate filter. Considering the term in Equation (10)

$$\begin{aligned} G_d(j\omega_i) - n(j\omega_i) &= G_{dr}(\omega) + jG_{di}(\omega) - [\bar{b} \bar{C}_N(\omega) - j \bar{b} \bar{S}_N(\omega)] \\ &= G_{dr}(\omega) - \bar{b} \bar{C}_N(\omega) + j[G_{di}(\omega) + \bar{b} \bar{S}_N(\omega)] \\ &= B_r(\omega) + jB_i(\omega) \end{aligned}$$

$$B_r = G_{dr}(\omega) - \bar{b} \bar{C}_N(\omega) \quad \text{and} \quad B_i = G_{di}(\omega) + \bar{b} \bar{S}_N(\omega) \quad (12)$$

Then, substituting in Equation (10), we get

$$\min_b \alpha$$

$$ST \begin{pmatrix} -\alpha & W(\omega_i)^* [B_r(\omega_i) + jB_i(\omega_i)]^* \\ W(\omega_i) [B_r(\omega_i) + jB_i(\omega_i)] & -1 \end{pmatrix} < 0 \quad (13)$$

for $\omega_i = i\Delta\omega$, $i = 0, \dots, L$, $\Delta\omega = \pi / L$.

In order to convert the above to a real LMI, we need the following Lemma.

Lemma 1

A complex hermitian matrix $H = H_R + jH_I$ satisfies

$$H \geq 0 \Leftrightarrow \begin{pmatrix} H_R & -H_I \\ H_I & H_R \end{pmatrix} \geq 0$$

Now, the last step in making Equation (13) in the form of LOMP with real LMI constraint is to apply Lemma 1 to Equation (13) constraint as follows (assuming $W(\omega_i)$ to be real)

$$\begin{aligned}
 & \min_{\bar{b}} \alpha \\
 ST & \begin{pmatrix} -\alpha & W^*(\omega_i)B_r(\omega_i) & 0 & -W(\omega_i)^*B_i(\omega_i) \\ W(\omega_i)B_r(\omega_i) & -1 & -W(\omega_i)B_i(\omega_i) & 0 \\ 0 & W(\omega_i)^*B_i(\omega_i) & -\alpha & W^*(\omega_i)B_r(\omega_i) \\ W(\omega_i)B_i(\omega_i) & 0 & W(\omega_i)B_r(\omega_i) & -1 \end{pmatrix} < 0 \quad (14) \\
 for & \quad \omega_i = i\Delta\omega, \quad i = 0, \dots, L, \quad \Delta\omega = \pi / L.
 \end{aligned}$$

Now Equation (14) is a LOMP with real LMI constraint (actually it is L LMIs). By solving Equation (14), the optimal \bar{b} variable will be found which represents the coefficients of the approximate FIR filter $G(z)$ of order N . The size of each one of the LMIs is 4×4 .

For *approach 2*, assume that $d(z) = 1$ and $n(z) = b_0 + b_1z^{-1} + \dots + b_Nz^{-N}$, where N is the FIR filter order, then Equation (9) will be

$$\begin{aligned}
 & \min_{n_i} \alpha \\
 ST & \begin{pmatrix} -\alpha & W^*(\omega_i)(G_r(\omega_i) - n_r(\omega_i)) & W^*(\omega_i)(G_i(\omega_i) - n_i(\omega_i)) \\ W(\omega_i)(G_r(\omega_i) - n_r(\omega_i)) & -1 & 0 \\ W(\omega_i)(G_i(\omega_i) - n_i(\omega_i)) & 0 & -1 \end{pmatrix} < 0, \quad (15) \\
 for & \quad \omega_i = i\Delta\omega, \quad i = 0, \dots, L, \quad \Delta\omega = \pi / L.
 \end{aligned}$$

Now by considering the value of $n(j\omega)$ from Equation (11)

$$\begin{aligned}
& \min_b \alpha \\
& ST \begin{pmatrix} -\alpha & \mathcal{W}^*(\omega_i)(G_r(\omega_i) - \bar{b}\bar{C}_v(\omega_i)) & \mathcal{W}^*(\omega_i)(G_i(\omega_i) + \bar{b}\bar{S}_v(\omega_i)) \\ \mathcal{W}(\omega_i)(G_r(\omega_i) - \bar{b}\bar{C}_v(\omega_i)) & -1 & 0 \\ \mathcal{W}(\omega_i)(G_i(\omega_i) + \bar{b}\bar{S}_v(\omega_i)) & 0 & -1 \end{pmatrix} < 0 \quad (16) \\
& \text{for } \omega_i = i\Delta\omega, \quad i=0, \dots, L, \quad \Delta\omega = \pi/L
\end{aligned}$$

The resulting LMIs from *approach 2* are of 3×3 size, which will give better computation time than *approach 1*. Hence, only *approach 2* LMIs will be used for computational purposes. By using LMI toolbox [29] (MATLAB® toolbox) Equation (16) and Equation (14) can be solved to find the global L_∞ Optimal Filter. Results will be illustrated with examples later in Chapter 4.

3.3 The IIR case

For the IIR case, only *approach 2* will be considered for its computational advantage. Starting from Equation (9), and by temporarily ignoring the presence of the nonlinear term $-\alpha d(j\omega)d^*(j\omega)$, $d(j\omega)$ can be represented as

$$\begin{aligned}
d(e^{j\omega}) &= 1 + a_1(\cos \omega - j \sin \omega) + a_2(\cos 2\omega - j \sin 2\omega) + \dots + a_M(\cos M\omega - j \sin M\omega) \\
&= (1 + a_1 \cos \omega + a_2 \cos 2\omega + \dots + a_M \cos M\omega) - j(a_1 \sin \omega + a_2 \sin 2\omega + \dots + a_M \sin M\omega)
\end{aligned}$$

Then,

$$\text{Re}(d(e^{j\omega})) = d_r(\omega) = 1 + \begin{pmatrix} a_1 & a_2 & \dots & a_M \end{pmatrix} \begin{pmatrix} \cos \omega \\ \cos 2\omega \\ \vdots \\ \cos M\omega \end{pmatrix} = 1 + \bar{a}\bar{C}_M(\omega)$$

$$\text{Im}(d(e^{j\omega})) = d_i(\omega) = \begin{pmatrix} a_1 & a_2 & \cdots & a_M \end{pmatrix} \begin{pmatrix} \sin \omega \\ \sin 2\omega \\ \vdots \\ \sin M\omega \end{pmatrix} = \bar{a}\bar{S}_M(\omega)$$

$$d(e^{j\omega}) = 1 + \bar{a}\bar{C}_M(\omega) - j\bar{a}\bar{S}_M(\omega)$$

Now, keeping in mind that in Equation (9) we have

$$A(j\omega) = d(j\omega)G_d(j\omega).$$

Then,

$$A(\omega) = [G_{dr}(\omega) + jG_{di}(\omega)][1 + \bar{a}\bar{C}_M(\omega) - j\bar{a}\bar{S}_M(\omega)] \Rightarrow$$

$$A_r(\omega) = G_{dr}(\omega) + \bar{a}\bar{C}_M(\omega)G_{dr}(\omega) + \bar{a}\bar{S}_M(\omega)G_{di}(\omega)$$

$$A_i(\omega) = G_{di}(\omega) - \bar{a}\bar{S}_M(\omega)G_{dr}(\omega) + \bar{a}\bar{C}_M(\omega)G_{di}(\omega)$$

Simplifying more, let

$$\Phi(\omega) = \bar{C}_M(\omega)G_{dr}(\omega) + \bar{S}_M(\omega)G_{di}(\omega)$$

$$\Theta(\omega) = \bar{C}_M(\omega)G_{di}(\omega) - \bar{S}_M(\omega)G_{dr}(\omega)$$

Then,

$$A_r(\omega) = G_{dr}(\omega) + \bar{a}\Phi(\omega) \quad \text{and} \quad A_i(\omega) = G_{di}(\omega) + \bar{a}\Theta(\omega) \quad (17)$$

Now grouping terms from Equation (17) and Equation (11) into Equation (9), we get

$$\begin{aligned} & \min_{\bar{b}, \bar{a}} \alpha \\ & \text{s.t.} \begin{pmatrix} -\alpha d(j\omega_i)d^*(j\omega_i) & W(\omega_i)^*(.) & W^*(\omega_i)(.) \\ W(\omega_i)(G_{dr}(\omega_i) + \bar{a}\Phi(\omega_i) - \bar{b}\bar{C}_N(\omega_i)) & -1 & 0 \\ W(\omega_i)(G_{di}(\omega_i) + \bar{a}\Theta(\omega_i) + \bar{b}\bar{S}_N(\omega_i)) & 0 & -1 \end{pmatrix} < 0, \quad (18) \\ & \text{for } \omega_i = i\Delta\omega, \quad i = 0, \dots, L, \quad \Delta\omega = \pi / L. \end{aligned}$$

Again, the term $\alpha d(j\omega)d^*(j\omega)$ is a nonlinear term in Equation (18). To overcome this nonlinearity, we will use an iterative scheme that will assume the term $d(j\omega)d^*(j\omega)$ to be a constant within the iteration to find the initial optimal $d(\cdot)$ (since $d(\cdot)$ is a decision variable in other LMI terms of Equation (18)) and $n(\cdot)$. Then, in each iteration, the previous value of $d(\cdot)$ will be used to calculate $d(j\omega)d^*(j\omega)$ leaving the linear presence of $d(\cdot)$ in Equation (18) as a variable. Now, let $d_i(\cdot)$ be the i -th value of $d(\cdot)$. Define the error function to be

$$E_{i+1} = |d_{i+1}(\cdot) - d_i(\cdot)| / |d_{i+1}(\cdot)|$$

Then, iteration $i+2$ will not start if $E_{i+1}(\omega) \leq \delta$, where δ is the chosen minimum tolerable error. When E_{i+1} approaches δ , it is assumed that the resulting $d_{i+1}(\cdot)$ and $n_{i+1}(\cdot)$ coefficients are close enough to the optimal solution of Equation (18). Although, for all test examples solved during the development and production phases of the algorithm, $d(\cdot)$ converged to the optimal, however, convergence is still not guaranteed.

Since we are minimizing against L_∞ function set, sometimes we would expect the resulting filter to be unstable. For such cases, the unstable poles will be replaced by their images inside the unit circle.

$$P_{Unstable} = a_u \angle \theta_u \quad \rightarrow \quad P_{Stable} = \frac{1}{a_u} \angle \theta_u$$

Generally, the problem will be changed in a way where optimality is not touched. Adding an all pass function (with a gain of 1) can preserve optimality to the original problem constraint as follows:

$$\left\| |a_u| \left(\frac{z - P_{Unstable}}{z - P_{Stable}} \right) (G_d(z) - G(z)) \right\|_{\infty} < \gamma \quad \forall \omega$$

Since the introduction of this will change the phase characteristics of the desired filter, it good to recall the fact that usually designers care less about the desired filter characteristics phase when using IIR filter design techniques. The examples discussed later will shed more light on the effect of stabilizing an IIR optimal filter.

3.4 FIR-Based Power Spectrum Approximation

The basic assumption for the power spectrum Approximation problem in this section is the availability of the frequency response characteristics of the signal under estimation. Usually, the signal $x(n)$, $-\infty < n < \infty$, will be observed for limited number of points, then the FTT can be obtained using any of the classical estimation techniques. The rule is that the higher the number of $x(n)$ points we take the better the quality of the filter, however, the order of the estimated transfer function will also increase.

This section will start by giving frequency characteristics either in the form of a transfer function or as a sequence $G_d(\omega_k) = G_k$, $k = 0, \dots, L$ and $\omega_k \in [0, \pi]$. The assumption is that $G_d(\omega)$ is with a reasonable accuracy and higher order (number of coefficients) and the aim is to maintain the accuracy as much as possible by applying the classical techniques with less number of parameters. Even if the transfer function of the signal is given, the frequency response $G_d(\omega)$ will be generated and the derivation of the algorithm of this section will be based on the availability of $G_d(\omega)$.

3.4.1 Optimal Power Spectrum Approximation Problem (FIR)

Consider the discrete Power Spectrum characteristic $G_d(j\omega) = \hat{G}_d(j\omega)\hat{G}_d^*(j\omega) \geq 0$ and an associated weight function $W(\omega)$. The problem is to find the optimal $G(j\omega) = \hat{G}(j\omega)\hat{G}^*(j\omega) = n(j\omega)$ that solves

$$\begin{aligned} \min_{n(\cdot)} \quad & \gamma \\ \text{Subject to} \quad & \|W(\omega)(G_d(\omega) - G(j\omega))\|_{\infty} < \gamma \quad \forall \omega \end{aligned} \quad (19)$$

The model used for $G(j\omega) = n(j\omega)$ has the following symmetric, noncausal characteristics

$$n(z) = b_{\frac{N}{2}} z^{\frac{N}{2}} + b_{\frac{N}{2}-1} z^{\frac{N}{2}-1} + \dots + b_2 z^2 + b_1 z + b_0 + b_1 z^{-1} + b_2 z^{-2} + \dots + b_{\frac{N}{2}-1} z^{-\frac{N}{2}+1} + b_{\frac{N}{2}} z^{-\frac{N}{2}} \quad (20)$$

where,

$$\begin{aligned} n_1(z) &= b_0/2 + b_1 z^{-1} + b_2 z^{-2} + \dots + b_{\frac{N}{2}-1} z^{-\frac{N}{2}+1} + b_{\frac{N}{2}} z^{-\frac{N}{2}} \\ n_2(z) &= b_0/2 + b_1 z^1 + b_2 z^2 + \dots + b_{\frac{N}{2}-1} z^{\frac{N}{2}-1} + b_{\frac{N}{2}} z^{\frac{N}{2}} \end{aligned}$$

are the causal and noncausal parts of $n(j\omega)$ respectively. Number of coefficients to be estimated in Equation (19) is $N/2$. Hence, the choice of N should reflect the desire of reducing the number of coefficients coming from the classical estimate. Note that N by definition is even. Now, by utilizing the special structure of $n(j\omega)$, we get

$$n(e^{j\omega}) = 2b_{\frac{N}{2}} \cos\left(\frac{N}{2}\omega\right) + 2b_{\frac{N}{2}-1} \cos\left(\left(\frac{N}{2}-1\right)\omega\right) + \dots + 2b_2 \cos(2\omega) + 2b_1 \cos(\omega) + b_0$$

or in a vector form we can write

$$n(\omega) = \begin{bmatrix} b_{\frac{N}{2}} & b_{\frac{N}{2}-1} & \cdots & b_2 & b_1 & b_0 \end{bmatrix} \begin{bmatrix} 2\cos(\frac{N}{2}\omega) \\ 2\cos((\frac{N}{2}-1)\omega) \\ \vdots \\ 2\cos(2\omega) \\ 2\cos(\omega) \\ 1 \end{bmatrix} = \bar{b}_N \bar{C}_N(\omega)$$

Note that apart from redefining $n(j\omega)$, all assumptions for Equation (16) for the FIR filter design problem are still valid. Recalling Equation (16)

$$\begin{aligned} & \min_{\bar{b}} \alpha \\ & \text{s.t.} \begin{pmatrix} -\alpha & W^*(\omega_i)(G_r(\omega_i) - \bar{b}\bar{C}_N(\omega_i)) & W^*(\omega_i)(G_r(\omega_i) + \bar{b}\bar{S}_N(\omega_i)) \\ W(\omega_i)(G_r(\omega_i) - \bar{b}\bar{C}_N(\omega_i)) & -1 & 0 \\ W(\omega_i)(G_r(\omega_i) + \bar{b}\bar{S}_N(\omega_i)) & 0 & -1 \end{pmatrix} < 0, \\ & \text{for } \omega_i = i\Delta\omega, \quad i = 0, \dots, L, \quad \Delta\omega = \pi/L. \end{aligned}$$

The imaginary parts of both $G(\omega)$ and $n(\omega)$ are zero. Hence, Equation (16) will take the following form

$$\begin{aligned} & \min_{\bar{b}} \alpha \\ & \text{s.t.} \begin{pmatrix} -\alpha & W^*(\omega_i)(G(\omega_i) - \bar{b}\bar{C}_N(\omega_i)) \\ W(\omega_i)(G(\omega_i) - \bar{b}\bar{C}_N(\omega_i)) & -1 \end{pmatrix} < 0, \\ & \text{for } \omega_i = i\Delta\omega, \quad i = 0, \dots, L, \quad \Delta\omega = \pi/L. \end{aligned} \quad (21)$$

Now, by solving Equation (21) using LMI toolbox [29] (MATLAB[®] toolbox), the optimal (Global) \bar{b} will be found that will best approximate $G_d(\omega)$ and consequently,

estimate the power spectrum of $x(n)$ with acceptable accuracy and less parameters. In order to present the solution utilizing the symmetry imposed on the FIR model chosen, we will utilize the fact that $G(z) = n(z) = \hat{n}(z)\hat{n}(-z)$, where $\hat{n}(z)$ represents the stable part of $n(z)$ and $\hat{n}(-z)$ represents the unstable part of $n(z)$.

3.5 IIR-Based Power Spectrum Approximation

The assumptions we imposed on the FIR-Based power spectral approximation problem also apply to the IIR case. The only difference is the IIR derivation of the approximate model of $G_d(\omega)$.

3.5.1 Optimal Power Spectrum Approximation Problem (IIR)

Consider the discrete Power Spectrum characteristic $G_d(j\omega) = \hat{G}_d(j\omega)\hat{G}_d^(j\omega) \geq 0$ and an associated weight function $W(\omega)$. The problem is to find the optimal*

$$G(j\omega) = \hat{G}(j\omega)\hat{G}^*(j\omega) = \frac{n(j\omega)}{d(j\omega)} \text{ that solves}$$

$$\begin{aligned} \min_{n(d)} \quad & \gamma \\ \text{Subject to} \quad & \|W(G_d(\omega) - G(j\omega))\|_{\infty} < \gamma \quad \forall \omega \end{aligned} \quad (22)$$

The same FIR symmetric, nocausal model will be assumed for $n(j\omega)$.

$$n(e^{j\omega}) = b_{\frac{N}{2}}z^{\frac{N}{2}} + b_{\frac{N}{2}-1}z^{\frac{N}{2}-1} + \dots + b_2z^2 + b_1z + b_0 + b_1z^{-1} + b_2z^{-2} + \dots + b_{\frac{N}{2}-1}z^{-(\frac{N}{2}-1)} + b_{\frac{N}{2}}z^{-(\frac{N}{2})}$$

$$n(\omega) = \begin{bmatrix} b_{\frac{N}{2}} & b_{\frac{N}{2}-1} & \cdots & b_2 & b_1 & b_0 \end{bmatrix} \begin{bmatrix} 2 \cos(\frac{N}{2}\omega) \\ 2 \cos((\frac{N}{2}-1)\omega) \\ \vdots \\ 2 \cos(2\omega) \\ 2 \cos(\omega) \\ 1 \end{bmatrix} = \bar{b}_N \bar{C}_N(\omega)$$

Now, for $d(j\omega)$ also, assume the following symmetric, noncausal model.

$$d(e^{j\omega}) = z^{\frac{M}{2}} + a_{\frac{M}{2}-1} z^{\frac{M}{2}-1} + \cdots + a_2 z^2 + a_1 z + a_0 + a_1 z^{-1} + a_2 z^{-2} + \cdots + a_{\frac{M}{2}-1} z^{-(\frac{M}{2}-1)} + z^{-(\frac{M}{2})} \Rightarrow$$

$$d(e^{j\omega}) = 2 \cos(\frac{M}{2}\omega) + 2a_{\frac{M}{2}-1} \cos((\frac{M}{2}-1)\omega) + \cdots + 2a_2 \cos(2\omega) + 2a_1 \cos(\omega) + a_0 \Rightarrow$$

$$d(\omega) = 2 \cos(\frac{M}{2}\omega) + \begin{bmatrix} a_{\frac{N}{2}-1} & a_{\frac{N}{2}-2} & \cdots & a_1 & a_0 \end{bmatrix} \begin{bmatrix} 2 \cos((\frac{M}{2}-1)\omega) \\ 2 \cos((\frac{M}{2}-2)\omega) \\ \vdots \\ 2 \cos(\omega) \\ 1 \end{bmatrix} \Rightarrow$$

$$d(\omega) = 2 \cos(\frac{M}{2}\omega) + \bar{a}_M \bar{C}_M(\omega)$$

keeping in mind that M and N are even numbers by definition, and $M \geq N$.

Starting from Equation (9)

$$\min_{\alpha, d(\cdot)} \alpha$$

$$S.T. \begin{pmatrix} -\alpha d(j\omega_i) d^*(j\omega_i) & W'(\omega_i)(A_r(\omega_i) - n_r(\omega_i)) & W'(\omega_i)(A_i(\omega_i) - n_i(\omega_i)) \\ W(\omega_i)(A_r(\omega_i) - n_r(\omega_i)) & -1 & 0 \\ W(\omega_i)(A_i(\omega_i) - n_i(\omega_i)) & 0 & -1 \end{pmatrix} < 0, \quad (23)$$

for $\omega_i = i\Delta\omega$, $i=0, \dots, L$, $\Delta\omega = \pi/L$

where $A(j\omega) = d(j\omega)G_d(j\omega)$.

Now since, $A(j\omega)$ and $n(j\omega)$ are all real, Equation (23) will become

$$\min_{n(\cdot), d(\cdot)} \alpha$$

$$ST \left(\begin{array}{cc} -\alpha d(\omega_i) d^*(\omega_i) & W^*(\omega_i)(A(\omega_i) - n(\omega_i)) \\ W(\omega_i)(A(\omega_i) - n(\omega_i)) & -1 \end{array} \right) < 0,$$

$$\text{for } \omega_i = i\Delta\omega, \quad i = 0, \dots, L, \quad \Delta\omega = \pi / L.$$

where

$$A(\omega_i) = 2G_d(\omega_i) \cos\left(\frac{M}{2}\omega_i\right) + G_d(\omega_i)\bar{a}_M\bar{C}_M(\omega_i)$$

$$n(\omega_i) = \bar{b}_N\bar{C}_N(\omega_i)$$

Then we have the following final shape of the IIR power spectrum estimation problem

$$\min_{\bar{a}, \bar{b}} \alpha$$

$$ST \left(\begin{array}{cc} -\alpha d(\omega_i) d^*(\omega_i) & W^*(\omega_i)(\cdot) \\ W(\omega_i)[2G_d(\omega_i) \cos\left(\frac{M}{2}\omega_i\right) + G_d(\omega_i)\bar{a}_M\bar{C}_M(\omega_i) - \bar{b}_N\bar{C}_N(\omega_i)] & -1 \end{array} \right) < 0, \quad (24)$$

$$\text{for } \omega_i = i\Delta\omega, \quad i = 0, \dots, L, \quad \Delta\omega = \pi / L.$$

To overcome the nonlinearity $d(j\omega)d^*(j\omega)$, we will use the same iterative scheme that was used for the IIR filter design problem, where we assumed that $d(j\omega)d^*(j\omega)$ to be a constant within the iteration.

In order to present the solution utilizing the symmetry imposed on the IIR model chosen, we will utilize the fact that $G(z) = \hat{G}(z)\hat{G}(-z)$, where $\hat{G}(z)$ represents the stable part of $G(z)$ and $\hat{G}(-z)$ represent the unstable part of $G(z)$.

3.6 Frequency Selection Algorithm

The number of LMIs to solve in the FIR/IIR design problems is very crucial for the speed of convergence to the final optimal solution. Specifically, in the IIR filter design problem speed of convergence is very sensitive to the parameter L , which is the number of frequency points selected for optimization within the frequency range $[0, \pi]$. This means that L LMIs will be solved for convergence to the final solution. In order to keep L as small as possible only frequencies corresponding to the error peaks should be selected for minimization.

Most of the time the optimal error is observed to have $2r + 2$ or $2r + 2$ equal peaks (equiripples) [37], where r is the filter order. This property can be exploited in reducing the number of LMIs solved to achieve the optimal solution. Focusing on the frequencies where the peak errors are occurring can do this.

An algorithm that starts with a very small L can achieve this frequency selection. For FIR this L can be as small as r (the approximate filter order). For IIR, L would be as small as $2r + 2$ (the order of the numerator and the denominator respectively). Then, in each iteration, the algorithm will search for the frequencies associated with error peaks to create the selected frequency set ω_p . Those frequency points will be added to the next iteration as minimization points for the next iteration. To get those frequencies, $G_d(j\omega)$

should be evaluated for a dense frequency set $\Omega \in [0, \pi]$. The size of Ω can be as big as r^2 for the FIR case and around $(2r + 2)^2$ for the IIR case. The algorithm will stop when the approximation error γ is small enough. The algorithm will keep track of two iteration frequencies after which it will discard them while it will always remember frequencies generated from the first iteration. Generally the frequency selection algorithm will do the following:

Step 1: Solve the filter design problem using only $2r + 2$ (IIR) or r (FIR) frequency points.

Step 2: Find the peak frequencies from the error function $|G_d - G(j\omega)|$ and add them to the optimization set.

Step 3: Solve the filter design problem again.

Step 4: Stop if the optimal reached otherwise go to *step 2*.

Frequency Selection Algorithm

- 1- Set iteration number to $k = 1$.
- 2- Define δ as a very small number for stopping criteria.
- 3- Define $G_d(j\omega_i)$ for $\omega_i \in \Omega$ and $i = 0, \dots, 50 \times T$ where T is a number close to the number of decision variables.
- 4- Define $G_{db}(j\omega_i)$ where $G_{db}(j\omega_i)$ is the frequency response of the $L+1$ equispaced frequencies for $\omega_i \in \Lambda$ and $i = 0, \dots, L$.
- 5- Solve the Optimization Problem to get the optimal variables \bar{b} (FIR) or \bar{b} and \bar{a} (IIR), and γ_k .

- 6- Check whether $(\gamma_k - \gamma_{k-1}) / \gamma_k = \delta_\gamma$, if yes, **STOP**, else, continue.
- 7- Generate $G_{opt}(j\omega_i)$, $\omega_i \in \Omega$ using the current optimal decision variables \bar{b} and possibly \bar{a} .
- 8- Generate $E(\omega) = |G_d(j\omega) - G_{opt}(j\omega)|$.
- 9- Create the frequency set $\omega_p \in \Omega$.
- 10 Expand $G_{db}(j\omega_i)$ for $\omega_i \in \Lambda \cup \omega_p$
- 11- Solve the Optimization Problem again to get the optimal variables \bar{b} (FIR) or \bar{b} and \bar{a} (IIR), and γ_{k+1} .
- 12- If $k > 2$, remove the last ω_p set to keep only two iterations in memory.
- 13- Prepare for the next iteration by making $\gamma_k = \gamma_{k+1}$ and $k = k + 1$.
- 14- Go to step 6.

CHAPTER 4

EXAMPLES

4.1 Summary

The proposed algorithms have been applied to various examples and the results obtained are presented in this chapter. Each example will include objective, discussion about the results and comparison with the existing techniques, and figures illustrating the results.

4.2 FIR Filter Design

In this section, two examples will be introduced. The first example will use the Optimal LMI-Based FIR Filter Design technique without intelligent frequency selection to design a low pass filter. The second example will be a repetition of the first one but for a high pass filter with intelligent frequency selection.

4.2.1 Example 1

Consider the frequency characteristics of a linear phase low pass filter $G_d(j\omega)$ given in Figure 1 and Figure 2. The passband is $\omega_p \in [0, 0.3\pi]$, the stop band is $\omega_s \in [0.6\pi, \pi]$, and the transition band is $\omega_t \in (0.3\pi, 0.6\pi)$. The linear phase is $e^{-j\frac{N}{2}\omega}$, where $N=30$ is the

required optimal filter order. It is required to design an optimal FIR filter with order $N=30$ that will solve the following problem

$$\begin{aligned} \min_{n(.)} \quad & \gamma \\ \text{Subject To} \quad & \|W(\omega)(G_d(j\omega) - G(j\omega))\|_{\infty} < \gamma \quad \forall \omega \end{aligned}$$

where $W(\omega)$ is a weight function.

Example 1 Objective: The objective of this example is to apply the LMI-Based technique to a classical filter design problem. The LMI-Based solution is expected to converge to the global minimum produced by Remez algorithm. Moreover, the effect of the transition band weighting is highlighted.

Discussion and Results of Example 1: The LMI based algorithm uses $W(\omega)$ to give a weight for each band including the transition band. For the LMI-based technique, the program is given three different weights for the transition band. The results in Table 1 show the optimal solutions of the three cases. Following are the coefficients of the optimal solution obtained by applying the LMI based technique with very low weight assigned to the transition band.

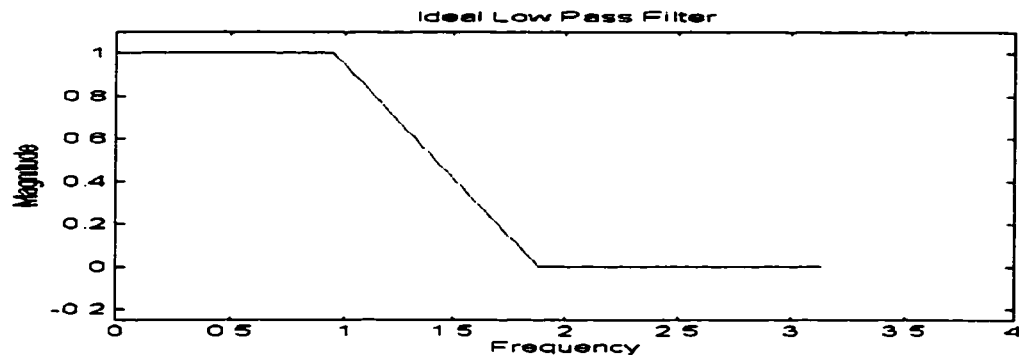


Figure 1 Ideal Low Pass Filter, Magnitude Frequency Characteristics for Example 1

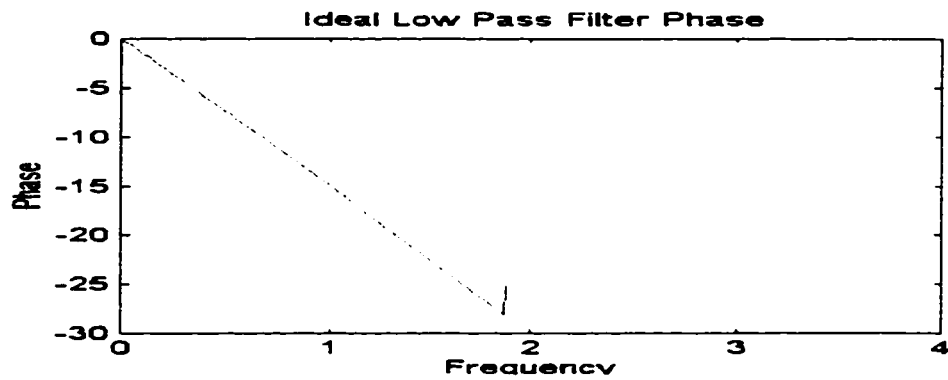


Figure 2 Ideal Low Pass Filter, Phase Frequency Characteristics for Example 1

	Tran. Band Weight	Tran. Band Error	Pass/Stop Band Error
Remez	zero	1.1087e-004	1.1087e-004
LMI	1 (No weight)	0.0120	0.0120
LMI	0.1	0.0026	0.511
LMI	0.0001	1.0374e-004	0.0021

Table 1 Weight Effect on Approximation Error, Example 1, FIR Case

$$B_{\text{optimal}} = [0.0002, 0.0006, -0.0007, -0.0025, 0.0007, 0.0070, 0.0018, -0.0148, -0.0104, \\ 0.0256, 0.0320, -0.0371, -0.0837, 0.0460, 0.3102, 0.4506, 0.3102, 0.0460, \\ -0.0837, -0.0371, 0.0320, 0.0256, -0.0104, -0.0148, 0.0018, 0.0070, 0.0007, \\ -0.0025, 0.0007, 0.0006, 0.0002].$$

The optimal filter produced by applying the LMI-based and the Remez algorithms will have the following zeros.

$$\text{Zeros}_{\text{optimal}} = [-2.0944, 1.7389 - 0.3364i, 1.7389 + 0.3364i, 1.4489 - 0.9356i, \\ 1.4489 + 0.9356i, 0.9051 - 1.3108i, 0.9051 + 1.3108i, -0.9939 - 0.1103i, \\ -0.9939 + 0.1103i, -0.9468 - 0.3218i, -0.9468 + 0.3218i, -0.8609 - 0.5087i, \\ -0.8609 + 0.5087i, -0.7474 - 0.6644i, -0.7474 + 0.6644i, -0.6187 - 0.7856i, \\ -0.6187 + 0.7856i, -0.4901 - 0.8717i, -0.4901 + 0.8717i, -0.3176 - 0.9482i, \\ -0.3176 + 0.9482i, -0.3816 - 0.9243i, -0.3816 + 0.9243i, 0.3567 - 0.5166i, \\ 0.3567 + 0.5166i, 0.4871 - 0.3145i, 0.4871 + 0.3145i, 0.5543 - 0.1072i, \\ 0.5543 + 0.1072i, -0.4775].$$

Figures of Example 1

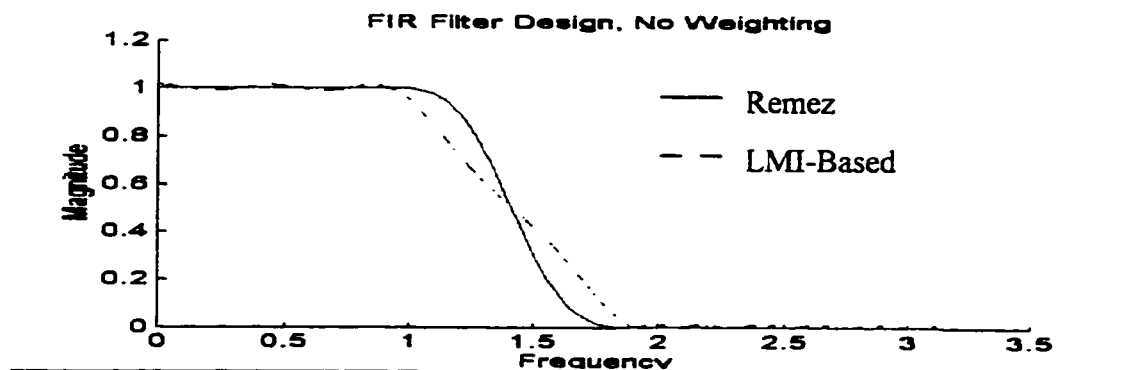


Figure 3 Remez vs LMI-Based, No Weight for T. Band, Example 1

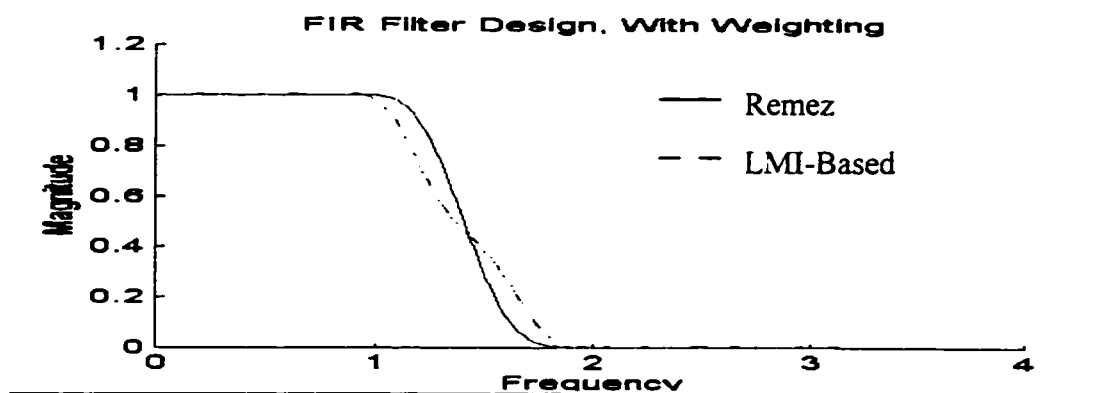


Figure 4 Remez vs LMI-Based, 0.1 weight for T. Band, Example 1

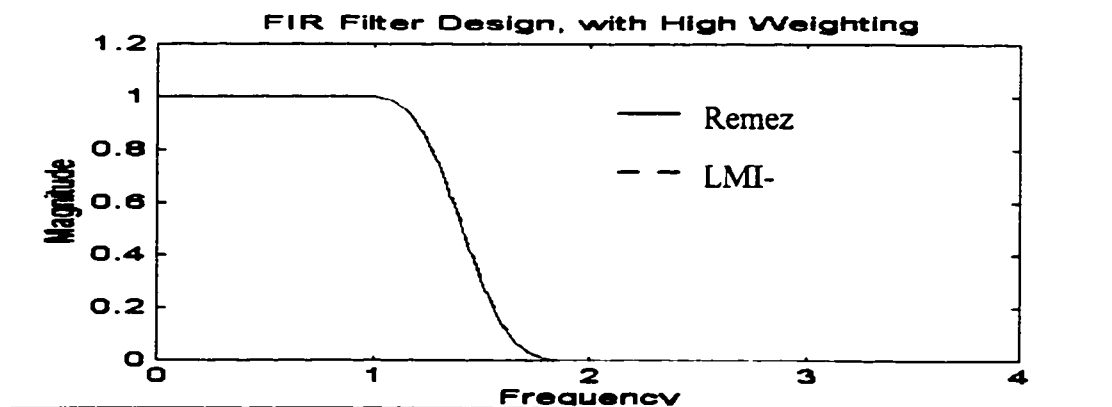


Figure 5 Remez vs LMI-Based, 0.0001 weight for T. Band, Example 1

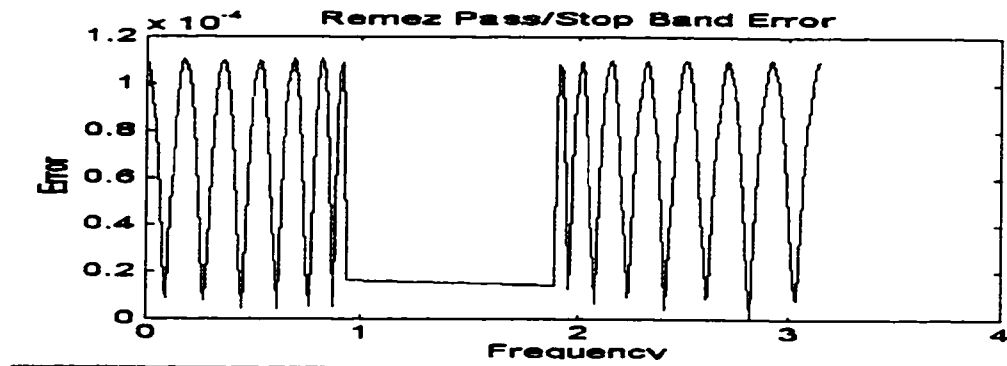


Figure 6 Remez Error Over the Pass/Stop Bands

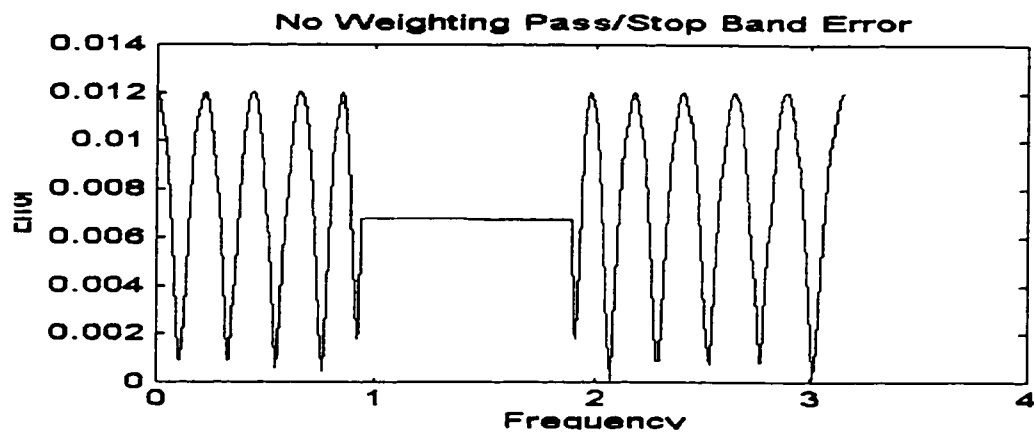


Figure 7 LMI-Based Error, No Weight

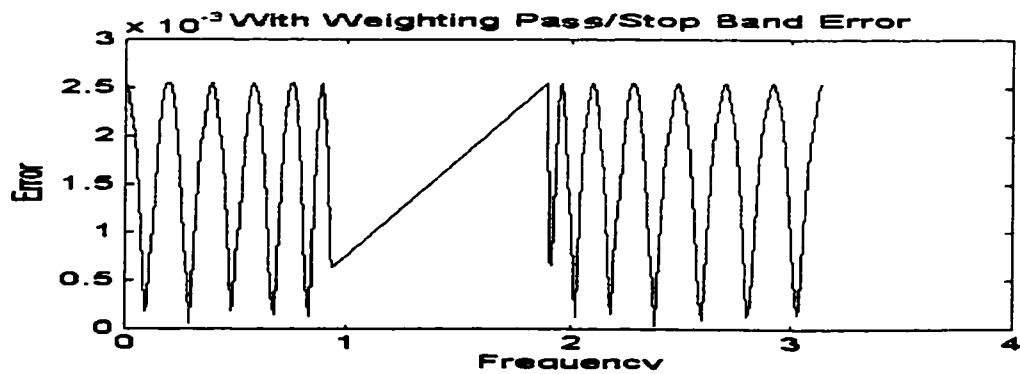


Figure 8 LMI-Based Error, 0.1 Weight

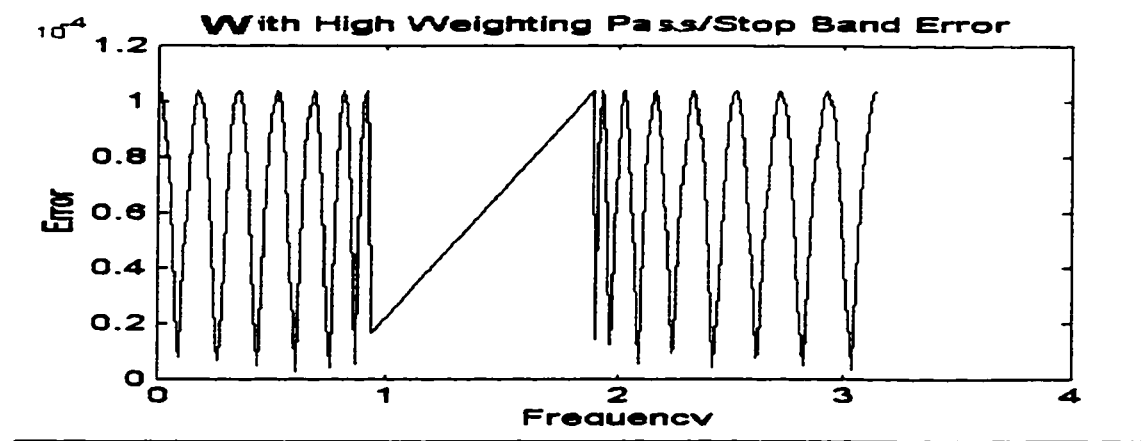


Figure 9 LMI-Based Error, 0.0001 Weight

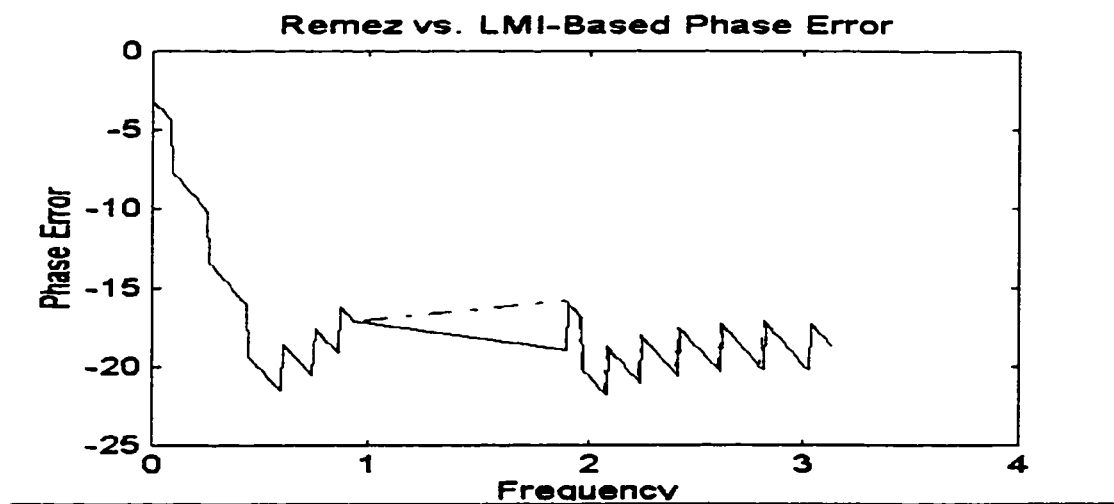


Figure 10 Remez vs LMI-Based Phase Error

4.2.2 Example 2

Consider the frequency characteristics of a linear phase high pass filter $G_d(j\omega)$ given in Figure 11 and Figure 12. The stopband is $\omega_s \in [0, 0.4\pi]$, the passband is $\omega_p \in [0.6\pi, \pi]$, and the transition band is $\omega_t \in (0.4\pi, 0.6\pi)$. The linear phase is $e^{-j\frac{N}{2}\omega}$, where $N=24$ is the required optimal filter order. It is required to design an optimal FIR filter with order $N=24$ that will solve the following problem.

$$\begin{aligned} \min_{n(\cdot)} \quad & \gamma \\ \text{Subject To} \quad & \|W(\omega)(G_d(j\omega) - G(j\omega))\|_{\infty} < \gamma \quad \forall \omega \bullet \end{aligned}$$

where $W(\omega)$ is a weight function.

Example 2 Objective: The objective of this example is to apply the LMI-Based technique to a classical FIR filter design problem together with the Frequency Selection Algorithm. The algorithm is expected to reduce the number of LMIs solved which will lead to better convergence time to the optimal solution.

Discussion and Results of Example 2: The results for this example were obtained using the same core program of Example 1. However, the iterative algorithm was added to facilitate the number of frequency points added and/or deleted at each iteration. It was learnt from Example 1 to give very low weight to the transition band, and this will be the default for Example 2. The transition band was given a weight of 0.0001 for all the runs.

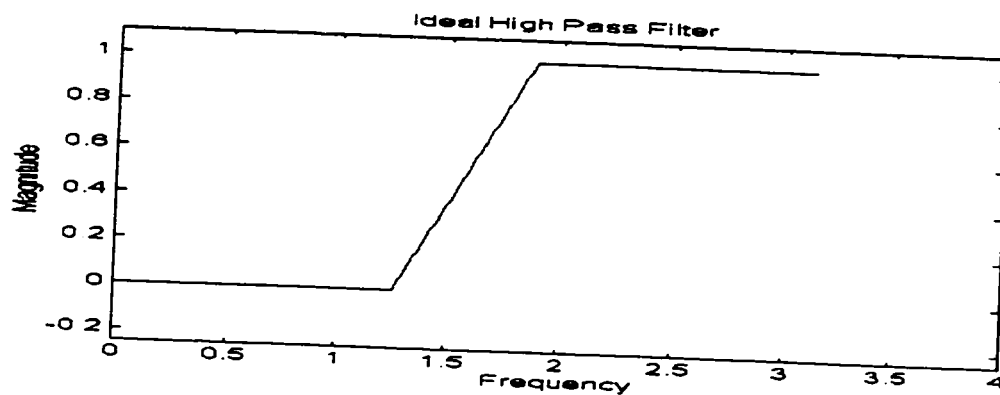


Figure 11 Ideal High Pass Filter, Frequency Mag. Characteristics for Example 2

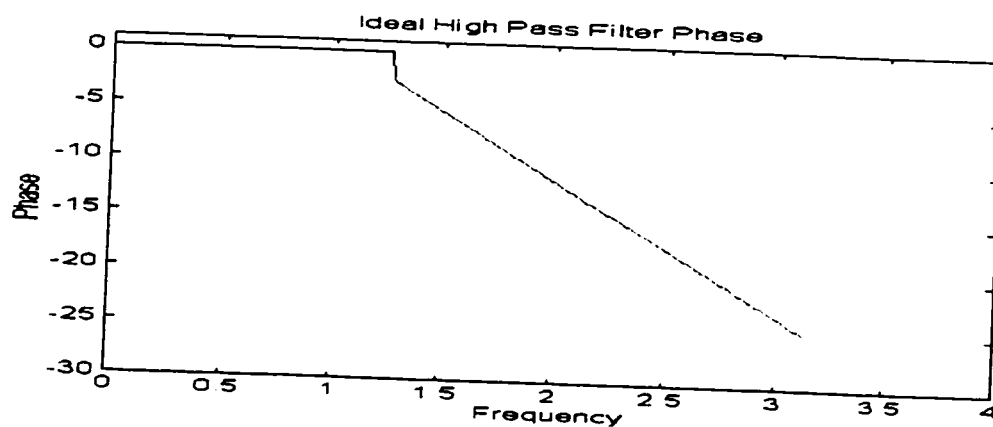


Figure 12 Ideal High Pass Filter, Phase Frequency Characteristics for Example 2

For the first run, the algorithm started with very low number of frequency points of 24, the same number as N (filter order). The algorithm kept a memory of two iterations while the first iteration always had N frequency points. After 3 iterations the algorithm converged to $\delta_\gamma = (\gamma_k - \gamma_{k-1}) / \gamma_k < 0.001$, after which the algorithm did not add any value to the problem by adding more peak frequencies. The coefficients produced by Remez and by the LMI-Based iterative schemes are listed below. Within the accuracy of 4 decimal points they are same.

$$\begin{aligned} B_{\text{LMI}} = [& 0.0000, 0.0072, 0.0000, -0.0136, 0.0000, 0.0263, 0.0000 \\ & -0.0486, 0.0000, 0.0965, 0.0000, -0.3150, 0.5000, -0.3150 \\ & 0.0000, 0.0965, 0.0000, -0.0486, 0.0000, 0.0263, 0.0000 \\ & -0.0136, 0.0000, 0.0072, 0.0000]. \end{aligned}$$

$$\begin{aligned} B_{\text{remez}} = [& 0.0000, 0.0072, 0.0000, -0.0136, 0.0000, 0.0263, 0.0000 \\ & -0.0486, 0.0000, 0.0965, 0.0000, -0.3150, 0.5000, -0.3150 \\ & 0.0000, 0.0965, 0.0000, -0.0486, 0.0000, 0.0263, 0.0000 \\ & -0.0136, 0.0000, 0.0072, 0.0000]. \end{aligned}$$

Table 2 explains clearly the effect of selecting the peak frequency on reducing the number of points required to reach the optimal solution. With only 56 points and 3 iterations the frequency selection algorithm reached to the required accuracy.

	No. Freq. Points	Tran. Band Weight	Tran. .Band Error	Pass/Stop Band Error
Remez	N/A	zero	0.0932	0.0056
LMI (with Iter.)	56	0.0001	0.0932	0.0055
LMI	56	0.0001	0.0933	0.0059
LMI	300	0.0001	0.0931	0.0055

Table 2 Number of Frequency Points Effect on Error, Example 1. FIR Case

Figures of Example 2

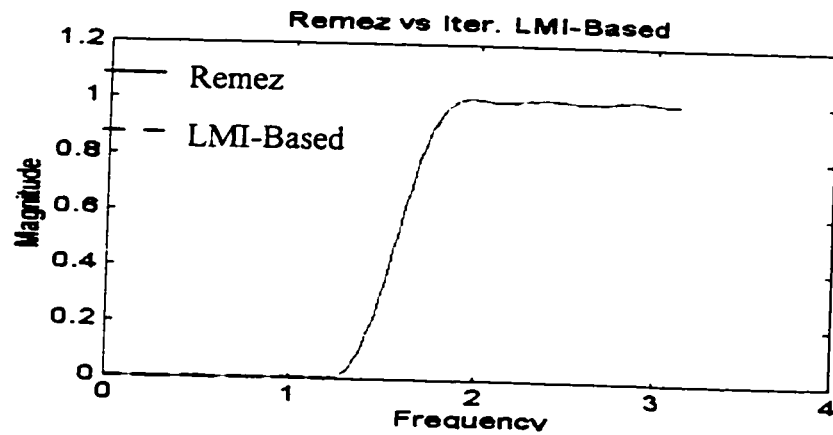


Figure 13 Remez vs LMI-Based with Frequency Selection

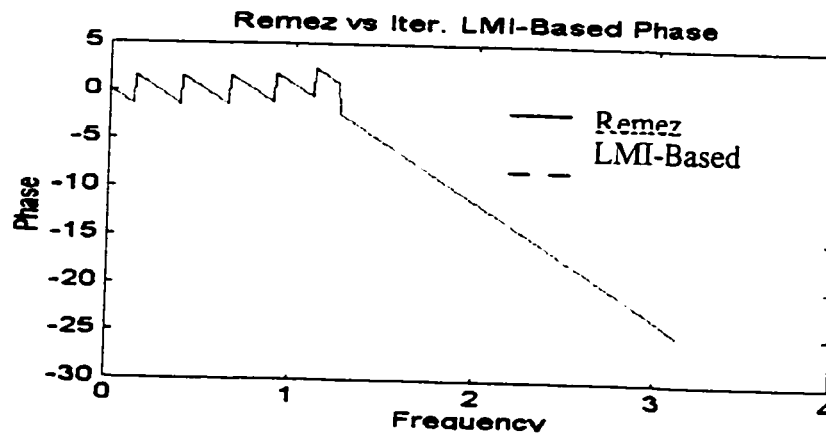


Figure 14 Remez vs LMI-Based with Frequency Selection, Phase

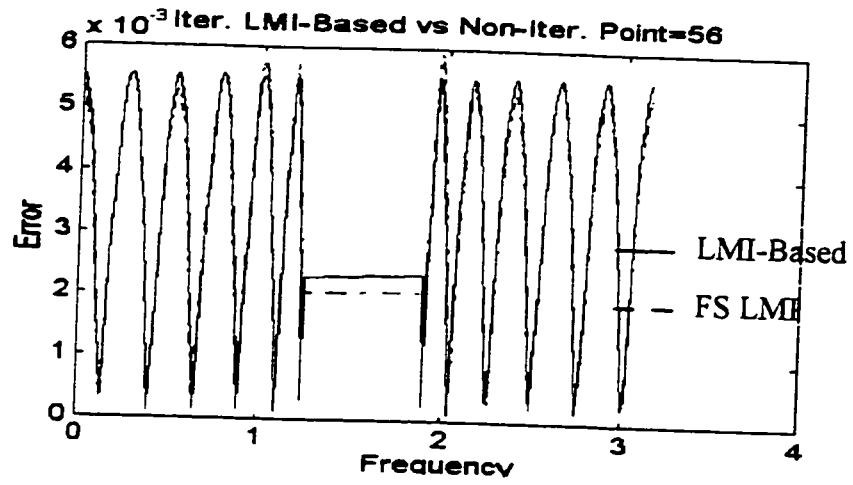


Figure 15 Frequency Selection Error vs Normal LMI-Based with 56 Points

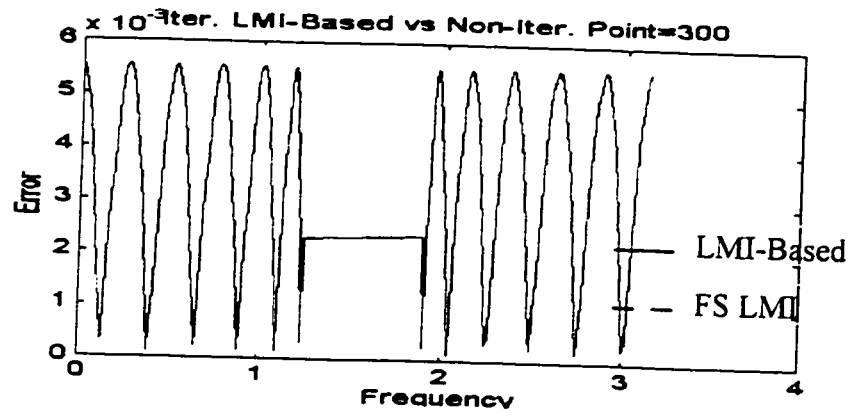


Figure 16 Frequency Selection Error vs Normal LMI-Based with 300 Points

4.3 IIR Filter Design

In this section, two examples will be introduced. The first example will use the Optimal LMI-Based IIR Filter Design technique without frequency selection to design a low pass filter. The second example will be a repetition for the first one but for a high pass filter with intelligent frequency selection.

4.3.1 Example 3

Consider the frequency characteristics of a linear phase low pass filter $G_d(j\omega)$ given in Figure 17 and Figure 18. The passband is $\omega_p \in [0, 0.3\pi]$, the stop band is $\omega_s \in [0.6\pi, \pi]$, and the transition band is $\omega_t \in (0.3\pi, 0.6\pi)$. The linear phase is $e^{-j\frac{N}{2}\omega}$, where $N=6$ is the required optimal filter order. It is required to design the optimal IIR filter with order $N=6$ that will solve the following problem.

$$\begin{aligned} \min_{n(\cdot), d(\cdot)} \quad & \gamma \\ \text{Subject To} \quad & \|W(\omega)(G_d(j\omega) - G(j\omega))\|_{\infty} < \gamma \quad \forall \omega \end{aligned}$$

where $W(\omega)$ is a weight function .

Example 3 Objective: The objective of this example is to apply the LMI-Based technique to a classical filter design problem and to compare it with *Yule Walker Least Squares Based Algorithm* and the *Elliptic Filter Design Algorithm*. The LMI-Based solution is expected to converge to an equi-ripple solution which will be compared with the *Yule Walker* and the *Elliptic* results. Moreover, the effect of the transition band weighting will be investigated. The phase approximation capabilities of the LMI-Based Technique will also be highlighted. Stability of the filter designed using the LMI-Based Technique will be discussed.

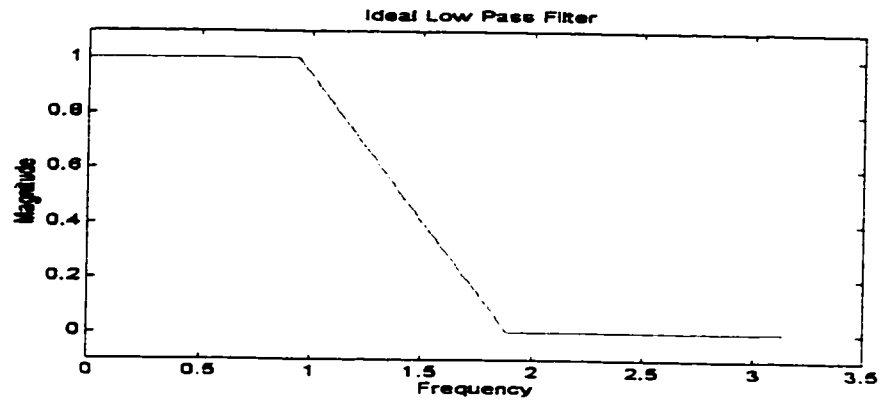


Figure 17 Ideal Low Pass Filter, Mag. Frequency Characteristics for Example 3

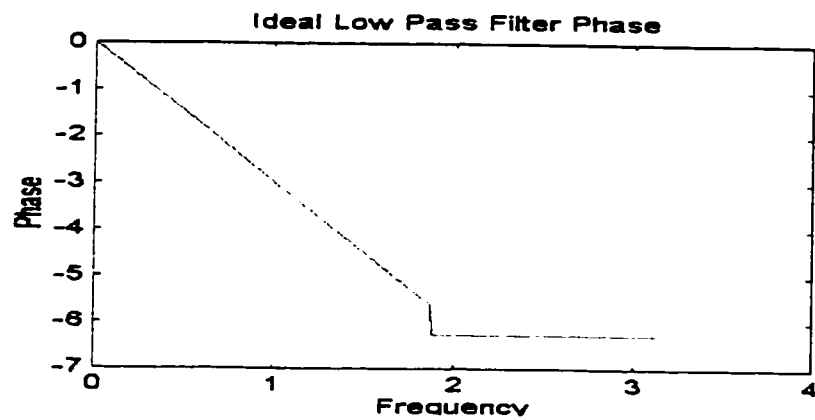


Figure 18 Ideal Low Pass Filter, Phase Frequency Characteristics for Example 3

Discussion and Results of Example 3: The results of applying the LMI-based techniques on Example 3 were first compared with the filter designed using *Yule Walker Least Squares Based Algorithm* [35]. The LMI based algorithm used $W(\omega)$ to give a weight for each band including the transition band. However, the specific program which was used to evaluate Yule Walker algorithm comes with MATLAB® Signal Processing Toolbox and treats all bands equally. *Yule Walker* algorithm produced the following coefficients that characterize the IIR filter.

$$\begin{aligned} B_{Yule} &= [0.1049 \quad 0.2215 \quad 0.2143 \quad 0.1049 \quad 0.0499 \quad 0.0621 \quad 0.0509]. \\ A_{Yule} &= [1.0000 \quad -1.0872 \quad 1.2325 \quad -0.7053 \quad 0.4744 \quad -0.1453 \quad 0.0395]. \\ \text{Poles}_{Yule} &= [-0.1103-0.6446i \quad -0.1103+0.6446i \quad 0.4316 - 0.5931i \quad 0.4316 + 0.5931i \\ &\quad 0.2223-0.3493i \quad 0.2223+0.3493i]. \end{aligned}$$

The results of LMI based technique were compared with those of *Elliptic Filter Design Algorithm* using the MATLAB® Signal Processing Toolbox function. The function was given the following parameters; Order = 6, $R_p=0.009$, $R_s=100$, Cut-off frequency = 0.3. The *Elliptic Filter Design Algorithm* produced the following coefficients that characterize the IIR filter.

$$\begin{aligned} B_{Ell} &= [0.0039 \quad 0.0180 \quad 0.0386 \quad 0.0490 \quad 0.0386 \quad 0.0180 \quad 0.0039]. \\ A_{Ell} &= [1.0000 \quad -2.6555 \quad 3.8330 \quad -3.3443 \quad 1.8479 \quad -0.6005 \quad 0.0896]. \\ \text{Poles}_{Ell} &= [-0.1103-0.6446i \quad -0.1103+0.6446i \quad 0.4316 - 0.5931i \quad 0.4316 + 0.5931i \\ &\quad 0.2223-0.3493i \quad 0.2223+0.3493i]. \end{aligned}$$

The LMI-Based Algorithm was started with $d(j\omega)=1$ as the initial choice of $d(\cdot)$. The number of frequency points were chosen to be 300 points. A weight of 0.01 was given to the transition band. In order to stop iterating for $d(\cdot)$, it was assumed that $E_{i+1}(\omega) \leq \delta = 0.01$ was enough to reach the required accuracy. With the above conditions, the LMI-Based algorithm converged to the following unstable optimal solution.

$$\begin{aligned}
B_{LMI} &= [-0.0162 \quad 0.0250 \quad 0.1417 \quad 0.2842 \quad 0.3166 \quad 0.2077 \quad 0.0752] \\
A_{LMI} &= [1.0000 \quad -1.3278 \quad 2.6047 \quad -2.3060 \quad 1.6013 \quad -0.6747 \quad 0.1397] \\
Poles_{LMI} &= [0.0700 + 1.1961i \quad 0.0700 - 1.1961i \quad 0.2028 + 0.6660i \quad 0.2028 - 0.6660i \\
&\quad 0.3910 + 0.2186i \quad 0.3910 - 0.2186i].
\end{aligned}$$

In order to stabilize the designed filter the following stabilizing gain and function were obtained from the two unstable poles.

$$\begin{aligned}
\text{Gain} &= 0.6966 \\
B_{\text{stabilizing}} &= [1.0000 \quad -0.1400 \quad 1.4356] \\
A_{\text{stabilizing}} &= [1.0000 \quad -0.0976 \quad 0.6966] \\
Poles_{\text{stabilizing}} &= [0.0488 - 0.8332i \quad 0.0488 + 0.8332i] \\
Zeros_{\text{stabilizing}} &= [0.0700 - 1.1961i \quad 0.0700 + 1.1961i]
\end{aligned}$$

By replacing the unstable poles with their image poles within the unit circle the following stable denominator and numerator were found.

$$\begin{aligned}
B_{LMI \text{ Stable}} &= [-0.0162 \quad 0.0250 \quad 0.1417 \quad 0.2842 \quad 0.3166 \quad 0.2077 \quad 0.0752] \\
A_{LMI \text{ Stable}} &= [1.0000 \quad -1.2853 \quad 1.8151 \quad -1.3856 \quad 0.8406 \quad -0.3303 \quad 0.0678] \\
Poles_{LMI \text{ Stable}} &= [0.0488 - 0.8332i \quad 0.0488 + 0.8332i \quad 0.2028 - 0.6660i \\
&\quad 0.2028 + 0.6660i \quad 0.3910 - 0.2186i \quad 0.3910 + 0.2186i]
\end{aligned}$$

Another LMI-Based run, but with no weight to any band, produced the following stable filter.

$$\begin{aligned}
B_{LMI \text{ No Weight}} &= [-0.0681 \quad 0.0631 \quad 0.2469 \quad 0.4688 \quad 0.4374 \quad 0.2489 \quad 0.0709] \\
A_{LMI \text{ No Weight}} &= [1.0000 \quad -0.1825 \quad 0.7847 \quad -0.3635 \quad 0.2196 \quad -0.0260 \quad -0.0217] \\
Poles_{LMI \text{ No Weight}} &= [-0.2390 - 0.8426i \quad -0.2390 + 0.8426i \quad 0.2439 - 0.5237i \\
&\quad 0.2439 + 0.5237i \quad 0.3898 - 0.2173i].
\end{aligned}$$

Table 3 analyzes the error of transition and the pass/stop bands. Both optimal solutions (with weight and without weight) are producing superior results compared with the *Yule Walker* and the *Elliptic* results. Both the *Yule Walker* and the *Elliptic* design algorithms ignore the desired phase characteristics and focus on the desired magnitude characteristics only. However, the LMI-Based algorithm takes into consideration both the magnitude and the phase of the desired characteristics. Given that the design error used to compare the ideal filter and the designed filter was chosen to be $Error = \left\| Mag_{desired} \angle Phase_{desired} - Mag_{designed} \angle Phase_{designed} \right\|$, the design error for the *Yule Walker* and the *Elliptic* filters will go high for the pass/stop bands. This is a direct result of including the phase in the error equation. Excluding the phase will show the excellent magnitude performance of the *Yule Walker* and the *Elliptic* filters, which is very much comparable with the LMI-Based filter (see figures 28 and 31).

The optimality of LMI-Based unstable solution can be maintained by altering the phase characteristics of the desired solution. Usually this is possible if the designer has flexible phased requirements for the designed filter which usually is the case with IIR filter design.

	Tran. Band Weight	Tran. .Band Error	Pass/Stop Band Error
Yule	1 (No weight)	1.1267	1.1322
Elliptic	1(No weight)	-	1.2
LMI	1 (No weight)	0.0420	0.0418
LMI _{unstable}	0.01	0.3015	0.003
LMI _{stable}	0.01	0.3015	0.003

Table 3 Weight & Stabilization Effect on Approximation Error, Example 3, IIR

Figures of Example 3

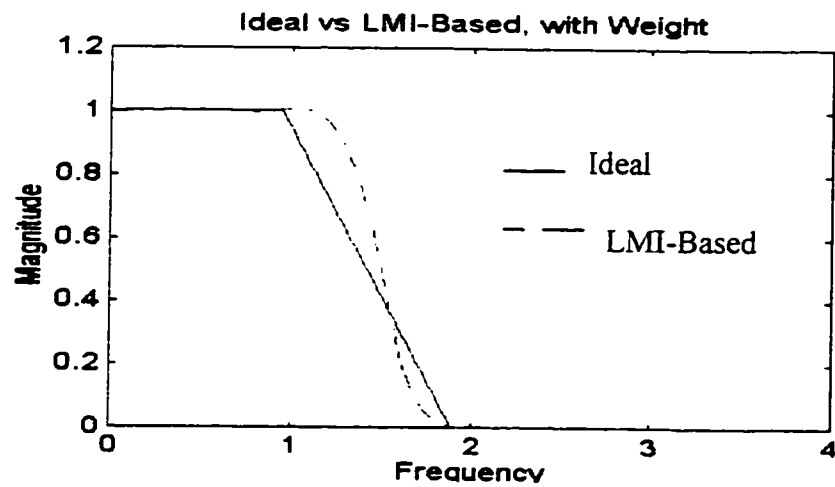


Figure 19 Ideal vs LMI-Based, with Weight for T.B, Unstable, Example 3

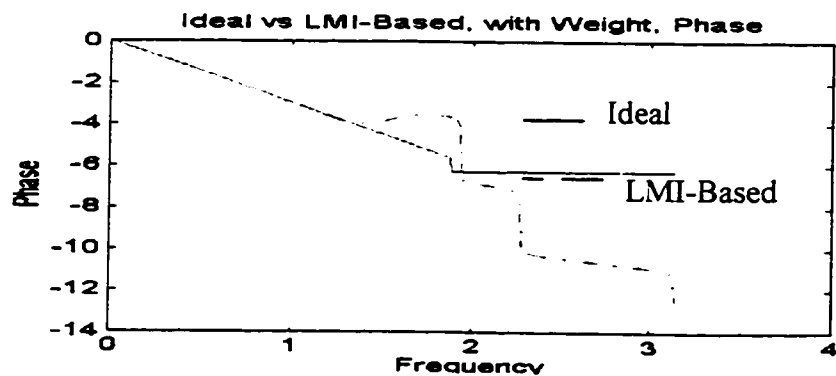


Figure 20 Ideal vs LMI-Based Phase, with Weight T.B, Unstable, Example 3

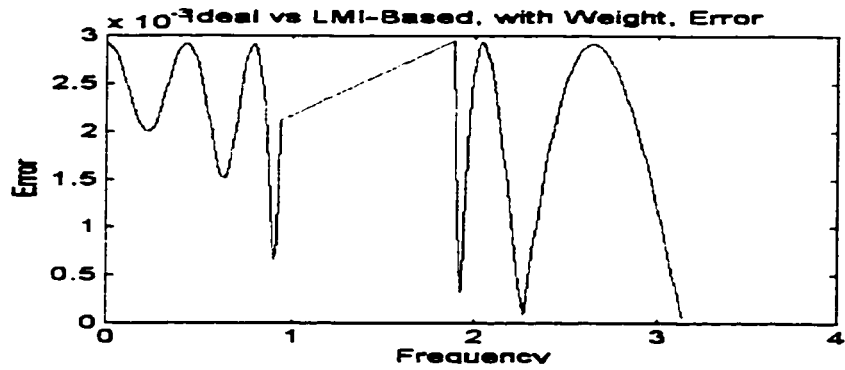


Figure 21 LMI-Based, with Weight, Unstable, Error for the Pass/Stop Bands

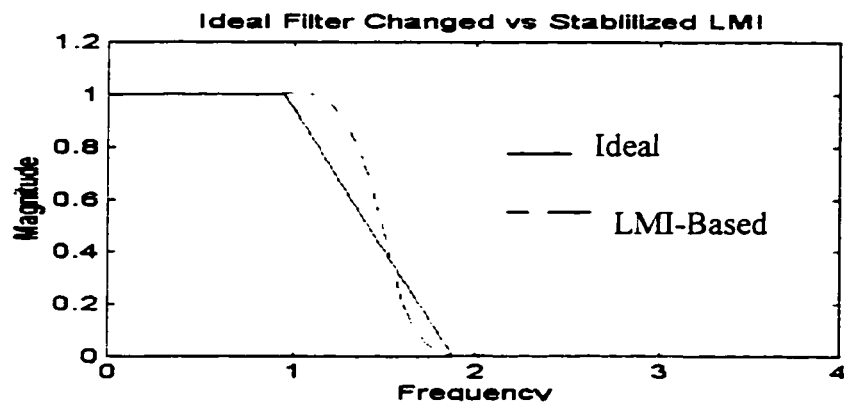


Figure 22 Ideal vs the Stabilized LMI-Based

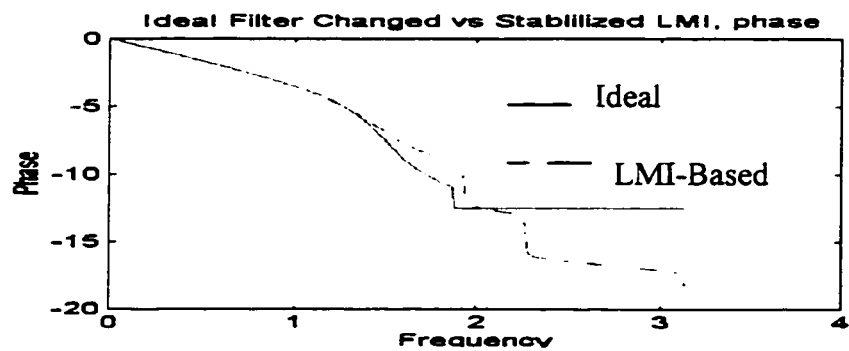


Figure 23 Ideal Phase vs the stabilized LMI-Based Phase

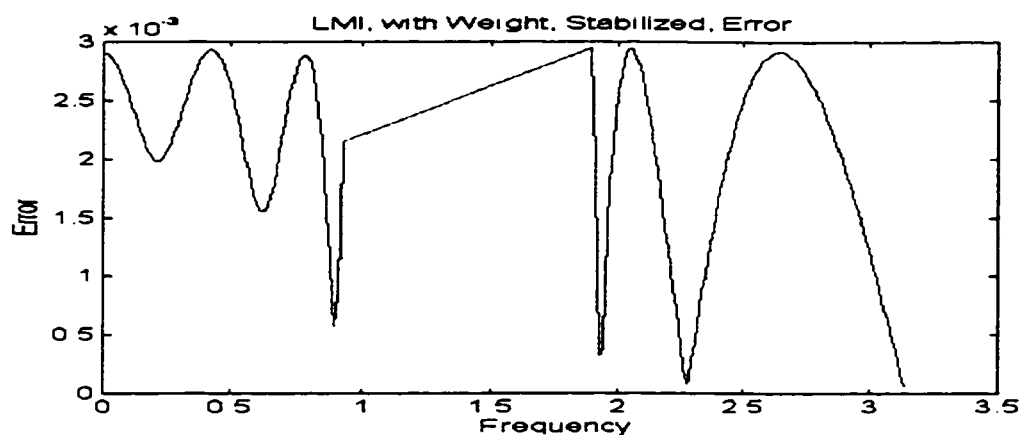


Figure 24 Error Between Ideal and Stabilized LMI-Based Fitters

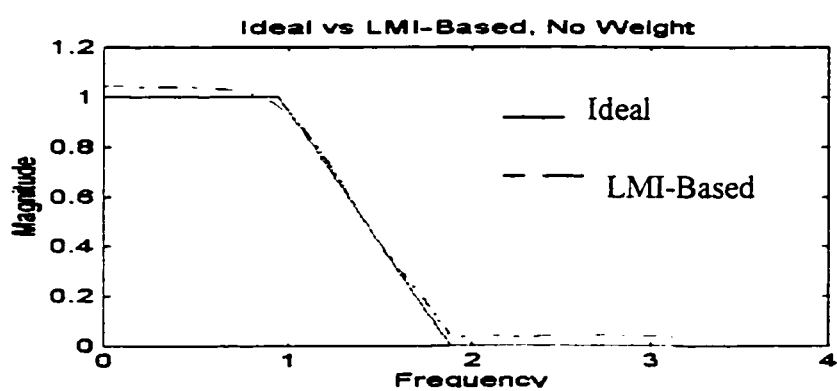


Figure 25 Ideal vs LMI-Based (Stable), with No Weight, Example 3

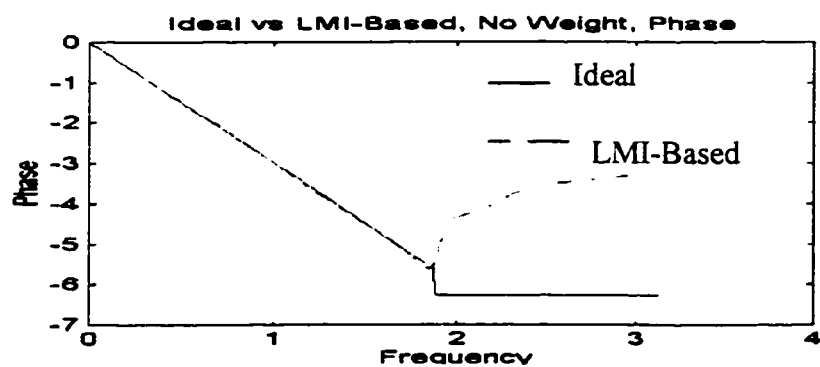


Figure 26 Ideal Phase vs LMI-Based (Stable), with No Weight, Example 3

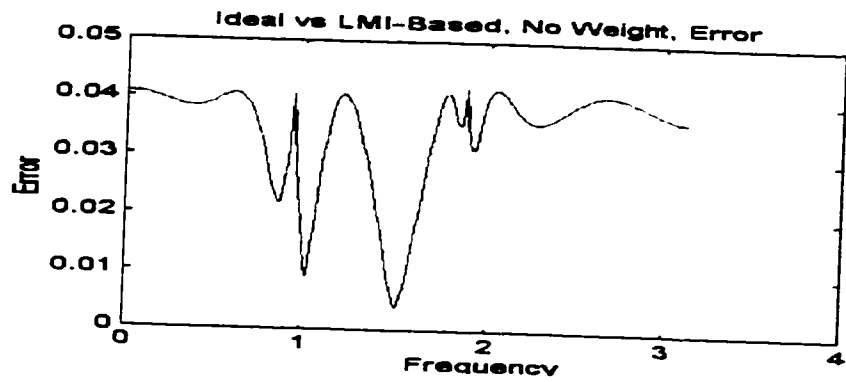


Figure 27 LMI-Based (Stable) Error Over All Bands

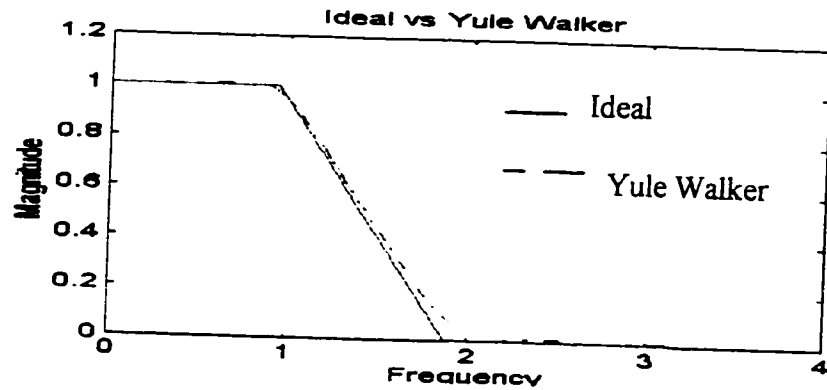


Figure 28 Ideal vs Yule Walker, Example 3

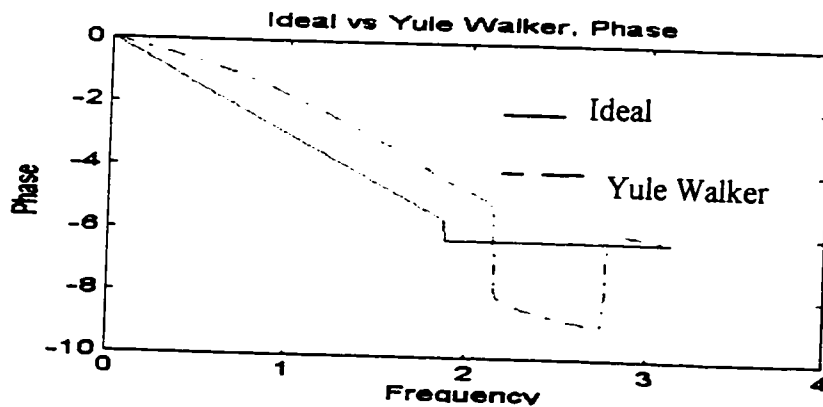


Figure 29 Ideal Phase vs Yule Walker Phase, Example 3

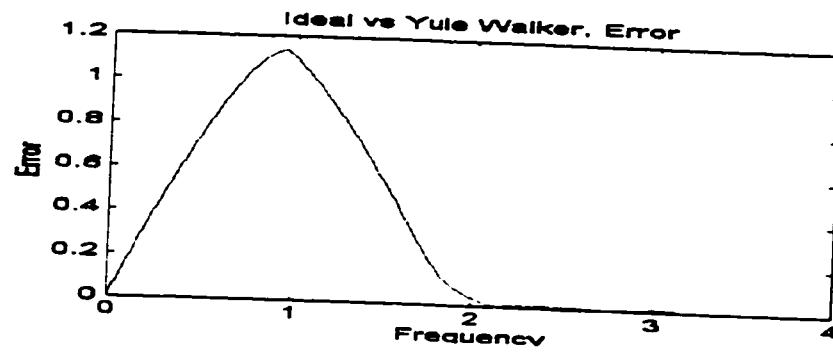


Figure 30 Yule Walker Error Over all Bands

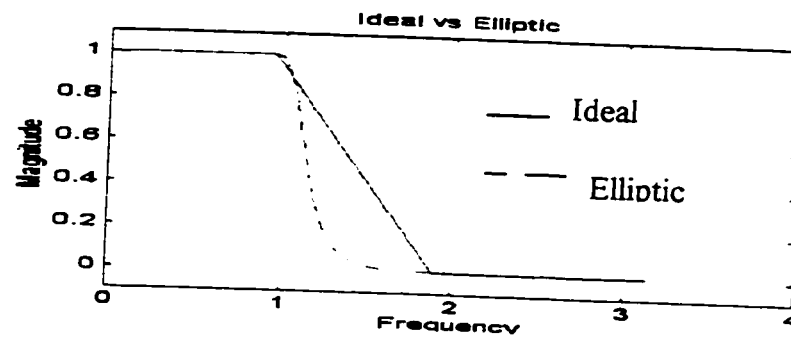


Figure 31 Ideal vs Elliptic, Example 3

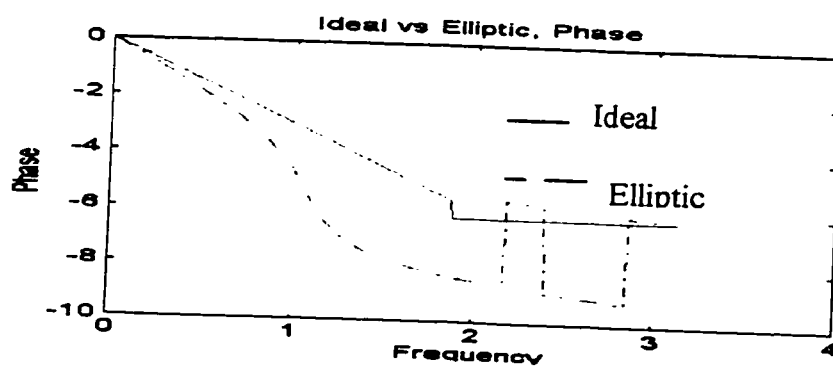


Figure 32 Ideal phase vs Elliptic phase, Example 3

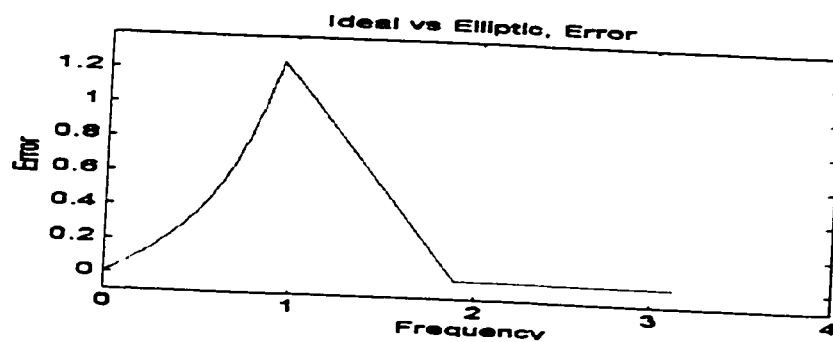


Figure 33 Elliptic Filter Error for the Pass & Stop Bands

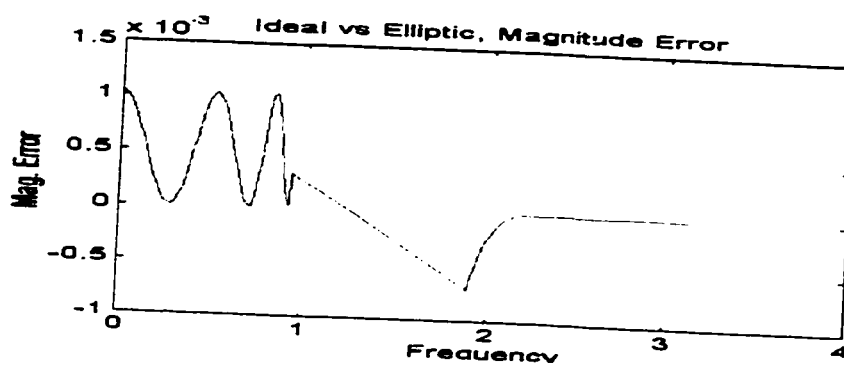


Figure 34 Elliptic Filter Magnitude Error over the Pass & Stop Bands

4.3.2 Example 4

Consider the frequency characteristics of a linear phase high pass filter $G_d(j\omega)$ given in Figure 35 and Figure 36. The stopband is $\omega_s \in [0, 0.4\pi]$, the passband is $\omega_p \in [0.6\pi, \pi]$, and the transition band is $\omega_t \in (0.4\pi, 0.6\pi)$. The linear phase is $e^{-j\frac{N+M}{2}\omega}$, where $N=M=8$ are the specified approximate filter numerator and denominator orders respectively. It is required to design the optimal IIR filter of order 8 that will solve the following problem.

$$\min_{n(\cdot), d(\cdot)} \gamma$$

$$\text{Subject To} \quad \|W(\omega)(G_d(j\omega) - G(j\omega))\|_{\infty} < \gamma \quad \forall \omega$$

where $W(\omega)$ is a weight function.

Example 4 Objective: The objective of this example is to apply the LMI-Based technique to a classical IIR filter design problem together with the Frequency Selection Algorithm. The algorithm is expected to reduce the number of LMIs solved to reach the optimal solution which will lead to less convergence time to reach the optimal solution. Moreover, the sensitivity of the LMI-Based algorithm to the initial choice of $d(\cdot)$ will be studied.

Discussion and Results of Example 4: The results for this example were obtained using the same core program of Example 3. However, the iterative algorithm was added to facilitate the number of frequency points added and/or deleted at each iteration. Unlike Example 3, no weight has been given to any of the bands.

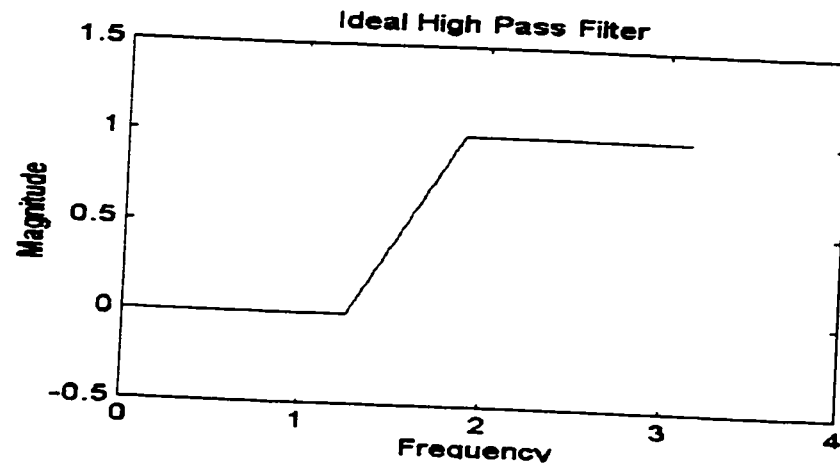


Figure 35 Ideal High Pass Filter, Frequency Mag. Characteristics for Example 4

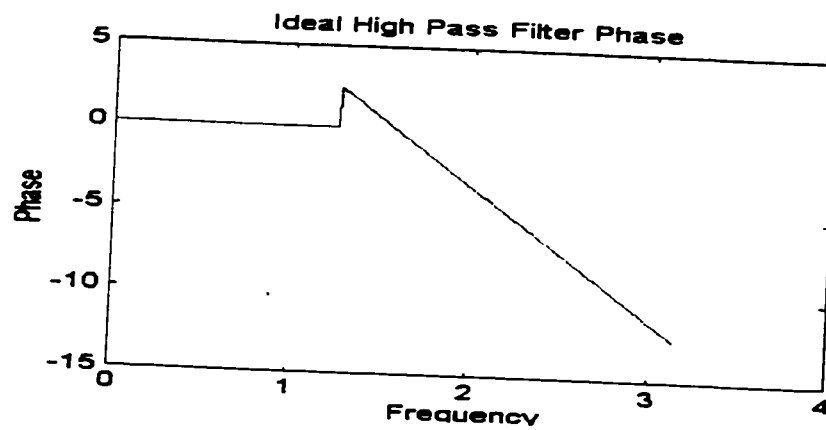


Figure 36 Ideal High Pass Filter, Phase Frequency Characteristics for Example

For the first run, the algorithm started with very low number of frequency points of 16 and $d(j\omega)=1$. In order to stop iterating for $d(\cdot)$, it was assumed that $E_{i+1}(\omega) \leq \delta = 0.01$ was enough to reach the required accuracy. The algorithm kept a memory of two iterations only while the first iteration always had N frequency points. After 7 iterations the algorithm converged to $\delta_\gamma = (\gamma_k - \gamma_{k-1}) / \gamma_k < 0.001$, after which the algorithm did not add any value to the problem by the peak frequencies added. The algorithm produced the following stable IIR filter with only 38 frequency points.

$$B_{\text{LMI}} = \begin{bmatrix} -0.0009 & 0.0147 & 0.0345 & 0.0114 & -0.0118 & 0.0501 & 0.1219 \\ -0.1018 & 0.1472 \end{bmatrix}.$$

$$A_{\text{LMI}} = \begin{bmatrix} 1.0000 & 1.9328 & 2.8179 & 3.0693 & 2.6278 & 1.7689 & 0.9025 \\ 0.3142 & 0.0611 \end{bmatrix}.$$

$$\text{Poles}_{\text{LMI}} = [0.1754-0.8462i \ 0.1754+0.8462i \ -0.1651-0.7191i \ -0.1651+0.7191i \\ -0.5963 - 0.2094i \ -0.5963 + 0.2094i \ -0.3803 - 0.4809i \ -0.3803 + 0.4809i].$$

Table 4 shows the effect of selecting the frequencies having the maximum error on the total no of the frequency points needed to achieve acceptable accuracy of the optimal solution.

Table 5 shows the minor effect the initial $d_i(\cdot)$ selection has on the optimal γ and the number of iterations needed for the algorithm (without frequency selection) to converge. The most important conclusion from Table 5 is the consistent convergence of the algorithm regardless of the initial $d_i(\cdot)$ chosen. Moreover, the table does not show any clear relation between the number of iterations taken to converge and the biasedness of initial $d_i(\cdot)$.

	No. Freq. Points	Tran. Band Weight	Tran. .Band Error	Pass/Stop Band Error
LMI (with iter.)	38	1	0.0255	0.0250
LMI	38	1	1.1419	2.0254
LMI	300	1	0.0252	0.0250

Table 4 No of Frequency Points Effect on T. & P/S Bands Errors, Example 4

	No. of Frequency Points	No of Iterations	$d_i(.)$ Error	γ
$d_i(.) = 1$	300	5	0.0047	
$d_i(.) = 1 + z^M$	300	6	0.0020	
$d_i(.)$ is the Elliptic Filter	300	5	0.0036	
$d_i(.)$ is random	300	4	0.0082	
$d_i(.)$ is random	300	5	0.0026	

Table 5 Algorithm sensitivity to initial d(.)

Figures of Example 4

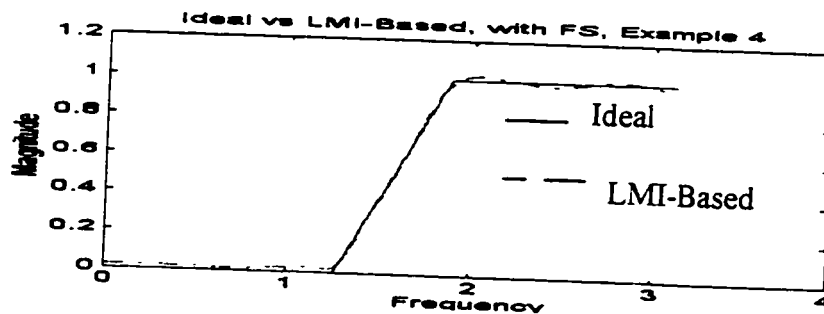


Figure 37 Ideal vs LMI Based with Freq. Selection

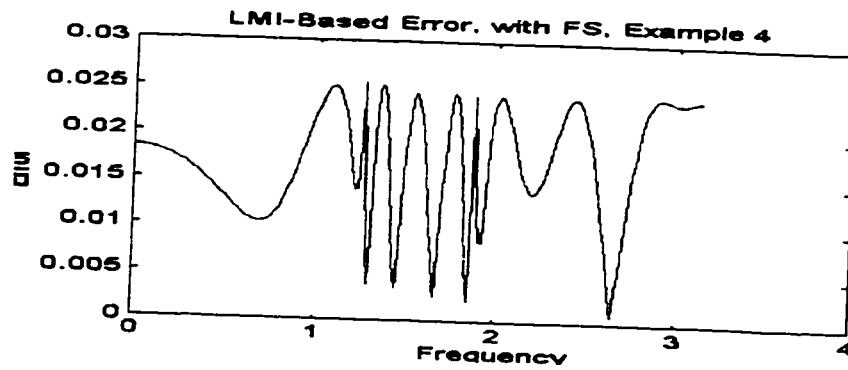


Figure 38 Error Between Ideal and LMI-Based with Freq. Selection

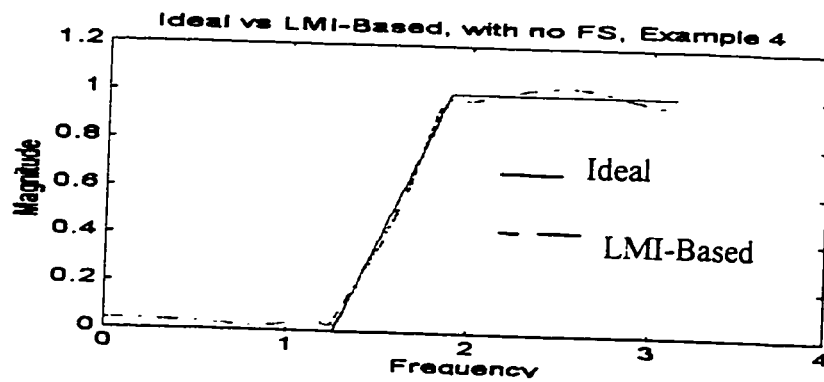


Figure 39 LMI-Based with no Freq. Selection $L=38$ vs Ideal

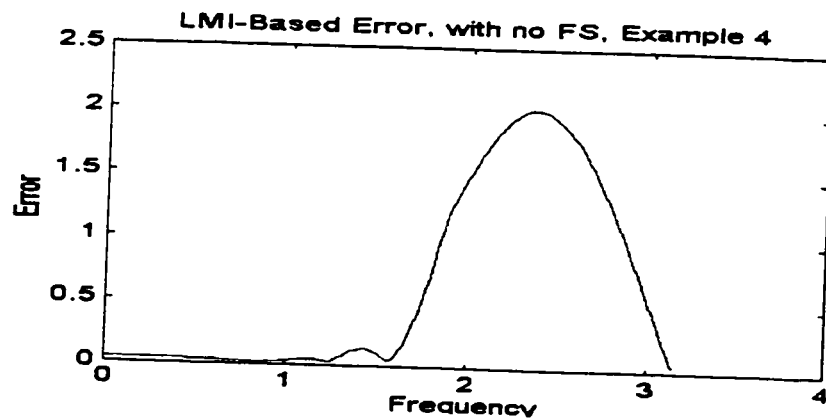


Figure 40 Error Between LMI-Based with no Freq. Selection and Ideal

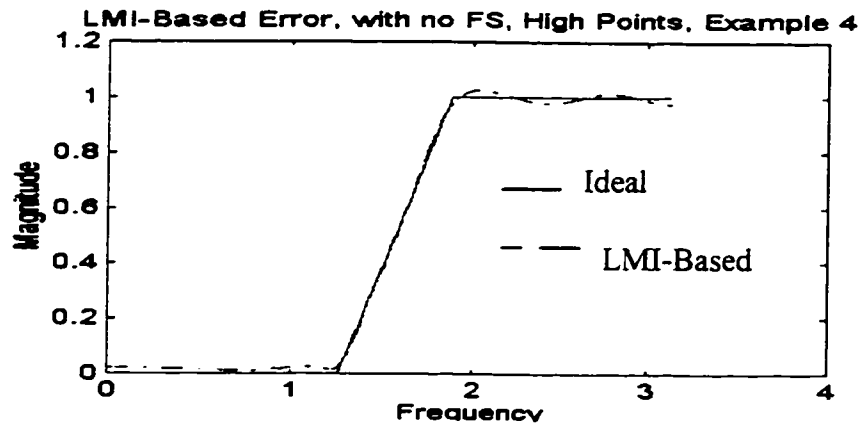


Figure 41 LMI-Based with No Freq. Selection $L=300$ vs Ideal

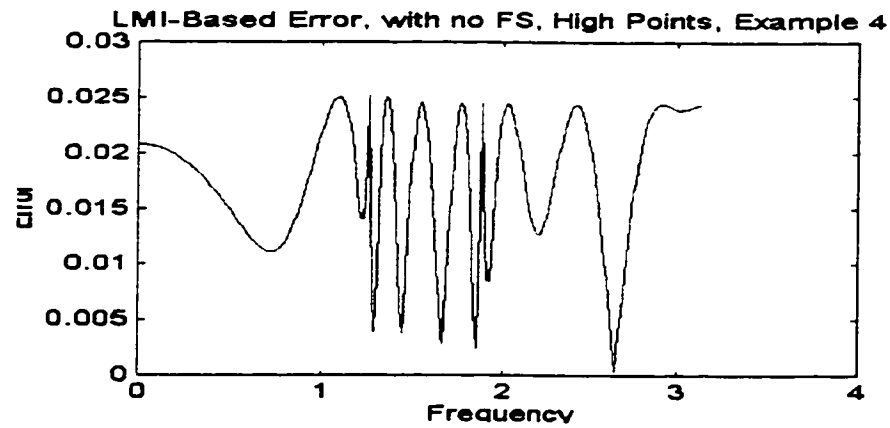


Figure 42 Error Between LMI-Based with no Freq. Selection $L=300$ and Ideal

4.4 Power Spectrum Estimation

In this section, two examples will be introduced. The first example will use the Optimal LMI-Based Power Spectrum Approximation technique with FIR as the model for approximating a given Power Spectrum Frequency Characteristic. The second example will be a repetition of the first one but with IIR as a model for approximation.

4.4.1 Example 5

Consider the frequency characteristics of a transfer function $G_d(j\omega)$ given in Figure 43. It is required to approximate $G_d(j\omega)$ with $G(j\omega) = n(j\omega)$ of order $N=20,16,12$ that will solve the following optimization problem.

$$\begin{aligned} \min_{n(\cdot)} \quad & \gamma \\ \text{Subject To} \quad & \|W(\omega)(G_d(j\omega) - G(j\omega))\|_{\infty} < \gamma \quad \forall \omega \end{aligned}$$

where $W(\omega)$ is a weight function .

Example 5 Objective: The objective of this example is to apply the LMI-Based Approximation technique to approximate a given Power Spectrum Frequency Characteristic. The approximation model will be FIR. The effect of order on the approximation error will be investigated.

Discussion and Results of Example 5: The LMI-Based algorithm was applied with three different FIR function orders $N = 20,16,12$. It is clear from Table 6 that higher the order we select for the approximation the more accuracy we get. The global optimal solutions are as follows.

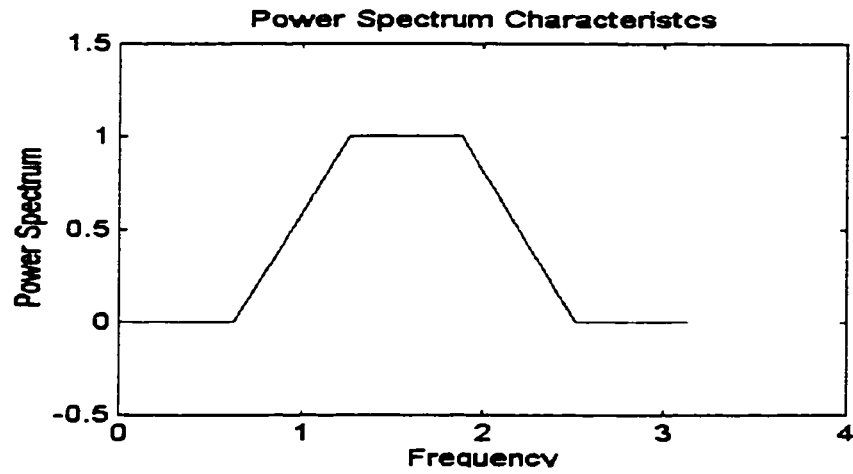


Figure 43 Power Spectrum Characteristics for Example 5

	No. Freq. Points	Approximation Order	Approximation Error
LMI-Based	500	20	0.0373
LMI-Based	500	16	0.0396
LMI-Based	500	12	0.0801

Table 6 The Effect of the Approximation Order on Error

$$B_{20} = \begin{bmatrix} -0.0029 & 0.0000 & -0.0191 & 0.0000 & 0.0331 & 0.0000 & 0.0810 \\ 0.0000 & -0.2806 & 0.0000 & 0.4129 & 0.0000 & -0.2806 & 0.0000 \\ 0.8100 & 0.0000 & 0.0331 & 0.0000 & -0.0191 & 0.0000 & -0.0029 \end{bmatrix}.$$

$$B_{16} = \begin{bmatrix} -0.0214 & 0.0000 & 0.0365 & 0.0000 & 0.0773 & 0.0000 & -0.2766 \\ 0.0000 & 0.4079 & 0.0000 & -0.2766 & 0.0000 & 0.0773 & 0.0000 \\ 0.3650 & 0.0000 & -0.0214 \end{bmatrix}.$$

$$B_{12} = \begin{bmatrix} 0.0217 & 0.0000 & 0.0820 & 0.0000 & -0.2718 & 0.0000 & 0.4160 \\ 0.0000 & -0.2718 & 0.0000 & 0.0820 & 0.0000 & 0.0217 \end{bmatrix}.$$

Then, by just selecting the stable (roots are inside the unit circle) part of each polynomial, we get.

$$BS_{20} = \begin{bmatrix} 1.0000 & 0.0010 & -1.2492 & 0.0007 & 0.9470 & -0.0003 & 0.0652 & -0.0002 \\ -0.1916 & 0.0000 & -0.0242 \end{bmatrix}$$

$$BS_{16} = \begin{bmatrix} 1.0000 & -0.0004 & -1.2637 & -0.0004 & 0.9605 & 0.0001 & 0.0818 & 0.0001 & -0.1874 \end{bmatrix}$$

$$BS_{12} = \begin{bmatrix} 1.0000 & 0.0017 & 4.9488 & 0.0122 & -7.4612 & 0.0106 & 6.2933 \end{bmatrix}$$

Figures of Example 5

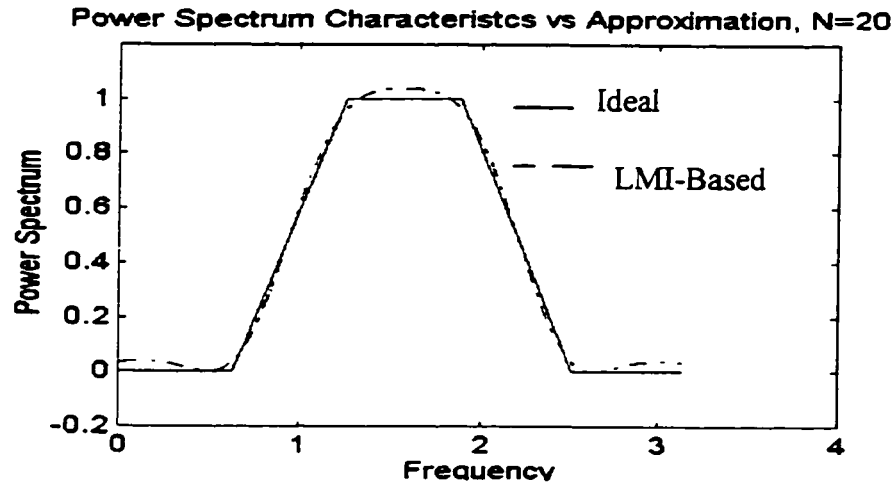


Figure 44 LMI-Based Approximation with N=20

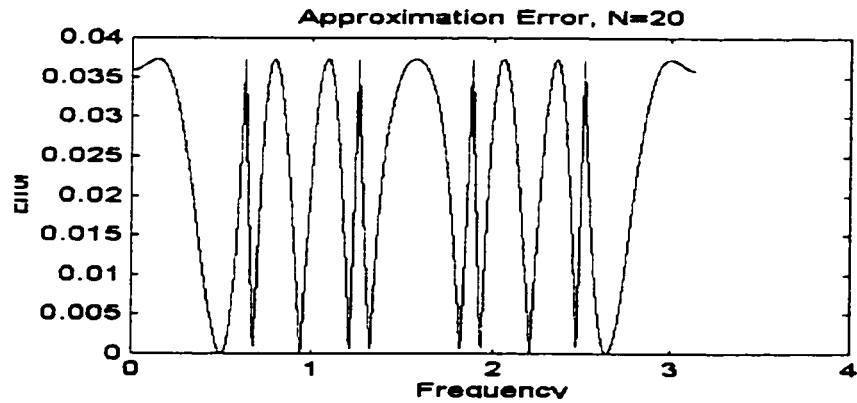


Figure 45 LMI-Based Approximation Error with N=20

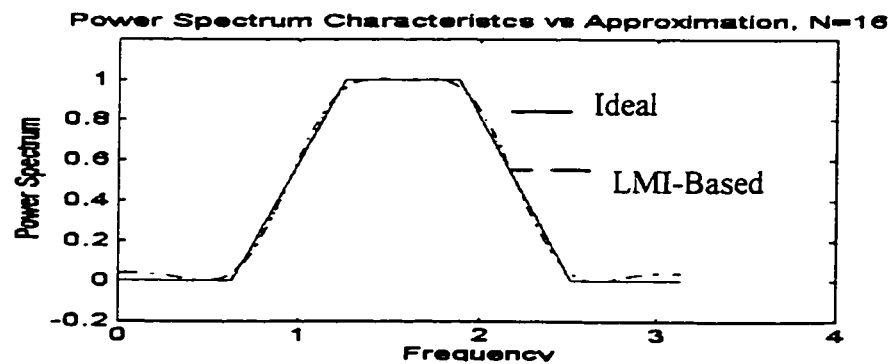


Figure 46 LMI-Based Approximation with N=16

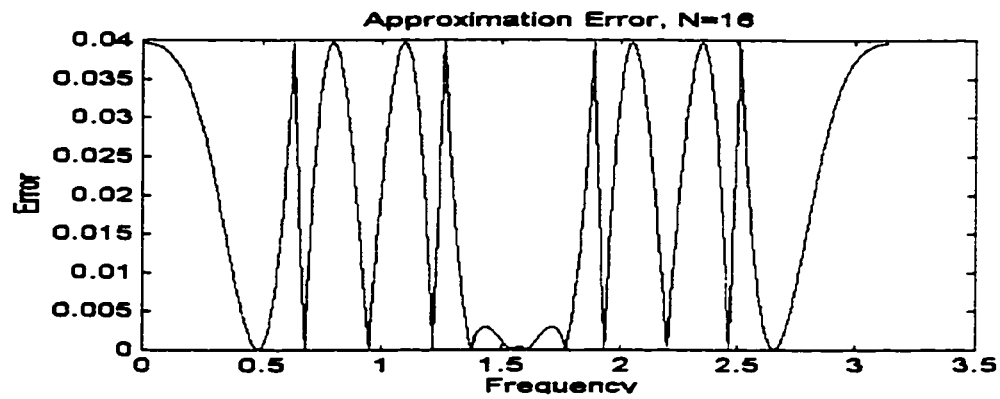


Figure 47 LMI-Based Approximation Error for N=16

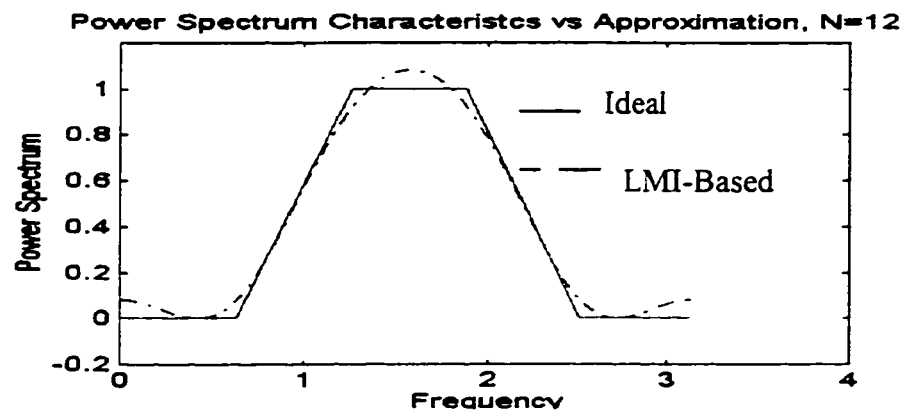


Figure 48 LMI-Based Approximation with N=12

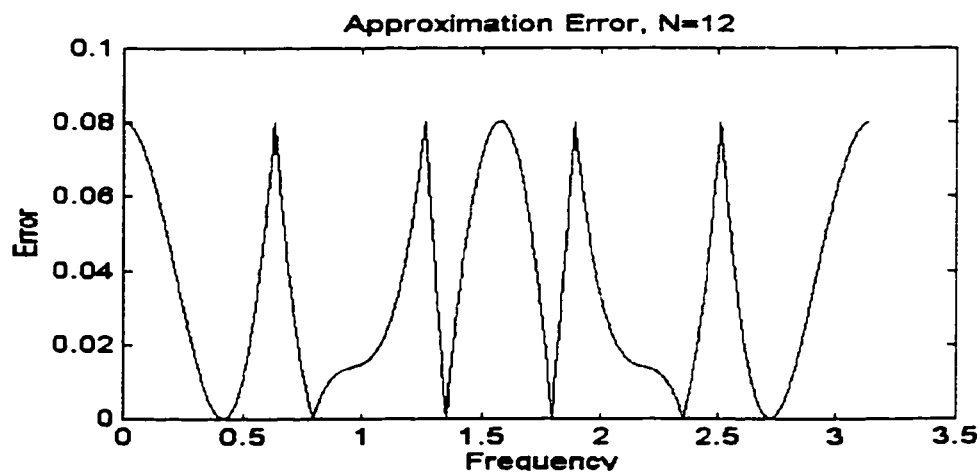


Figure 49 LMI-Based Approximation Error for N=12

4.4.2 Example 6

Consider the frequency characteristics of a transfer function $G_d(j\omega)$ given in Figure 50. It is required to approximate $G_d(j\omega)$ with $G(j\omega) = \frac{n(j\omega)}{d(j\omega)}$ of order $N=12,10,8$ that will solve the following optimization problem.

$$\begin{aligned} \min_{n(\cdot), d(\cdot)} \quad & \gamma \\ \text{Subject To} \quad & \|W(\omega)(G_d(j\omega) - G(j\omega))\|_{\infty} < \gamma \quad \forall \omega \end{aligned}$$

where $W(\omega)$ is a weight function .

Example 6 Objective: The objective of this example is to apply the LMI-Based Approximation technique to approximate a given Power Spectrum Frequency Characteristic. The approximation model will be IIR. The effect of order on the approximation error will be investigated.

Discussion and Results of Example 6: The LMI-Based algorithm was applied with three different IIR function orders $N = 14, 10, 8$. The choice was set to $E_{i+1}(\omega) \leq \delta = 0.01$ and the initial estimate of $d(\cdot)$ to $d(j\omega) = 1$. It is not very clear from Table 7 that the higher the order we select for the approximation the more accuracy we get. The global optimal solutions we got for approximation order 14 is

$$B_{14} = \begin{bmatrix} 0.9717 & 0.0010 & 3.8464 & 0.0027 & 6.8504 & 0.0030 & 7.7744 \\ 0.0024 & 7.7744 & 0.0030 & 6.8504 & 0.0027 & 3.8464 & 0.0010 \\ 0.9717 \end{bmatrix}.$$

$$A_{14} = \begin{bmatrix} 1.0000 & 0.0009 & 3.0552 & 0.0023 & 7.4255 & 0.0041 & 7.0285 \\ 0.0008 & 7.0285 & 0.0041 & 7.4255 & 0.0023 & 3.0552 & 0.0009 \\ 1.0000 \end{bmatrix}.$$

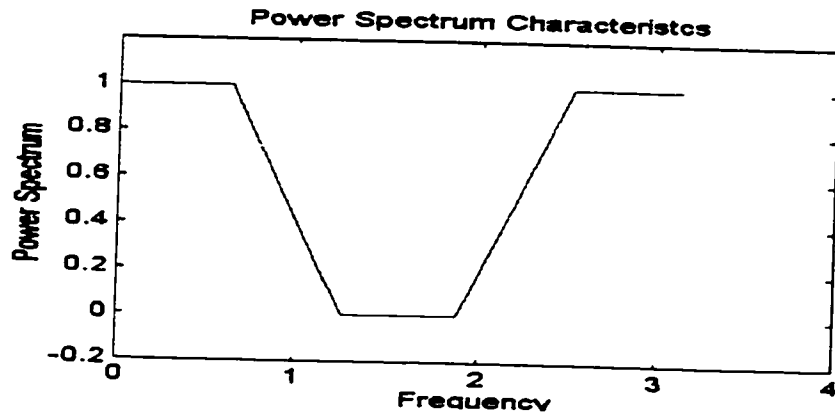


Figure 50 Power Spectrum Characteristics for Example 6

	No. Freq. Points	Approximation Order	Approximation Error
LMI-Based	500	14	0.0512
LMI-Based	500	10	0.0521
LMI-Based	500	8	0.0519

Table 7 The Effect of the Approximation Order on the Error

By doing 6 exact pole-zero cancellation between B_{14} and A_{14} , and by separating the stable part we will get the following polynomials.

$$BS_{14} = [1.0000 \ 0 \ 1.2847 \ 0.0000 \ 0.5621];$$

$$AS_{14} = [1.0000 \ 0 \ 0.4617 \ 0 \ 0.2094]$$

The 10th order approximation is:

$$B_{10} = [0.9594 \ 0.0000 \ 4.3767 \ 0.0001 \ 8.4762 \ 0.0002 \ 8.4762 \\ 0.0001 \ 4.3767 \ 0.0000 \ 0.9594].$$

$$A_{10} = [1.0000 \ 0.0000 \ 3.5977 \ 0.0001 \ 8.5352 \ 0.0002 \ 8.5352 \\ 0.0001 \ 3.5977 \ 0.0000 \ 1.0000].$$

By doing 2 exact pole-zero cancellation between B_{10} and A_{10} , and by separating the stable part we get the following polynomials.

$$B_{10} = [1.0000 \ 0 \ 1.2635 \ 0 \ 0.5497]$$

$$A_{10} = [1.0000 \ 0 \ 0.4511 \ 0 \ 0.2101]$$

For the 8th order approximation we get the following polynomials.

$$B_8 = [0.9616 \ 0.0000 \ 3.4275 \ 0.0000 \ 5.0724 \ 0.0000 \ 3.4275 \\ 0.0000 \ 0.9616].$$

$$A_8 = [1.0000 \ 0.0000 \ 2.6094 \ 0.0000 \ 5.9487 \ 0.0000 \ 2.6094 \\ 0.0000 \ 1.0000].$$

By taking the stable part also, we get

$$B_8 = [1.0000 \ 0 \ 1.2681 \ 0 \ 0.5522]$$

$$A_8 = [1.0000 \ 0.0000 \ 0.4529 \ 0.0000 \ 0.2100]$$

It is very clear that the approximation redundancy can be filtered out by very accurate pole-zero cancellation to get almost the same optimal approximation function for different orders.

Figures of Example 6

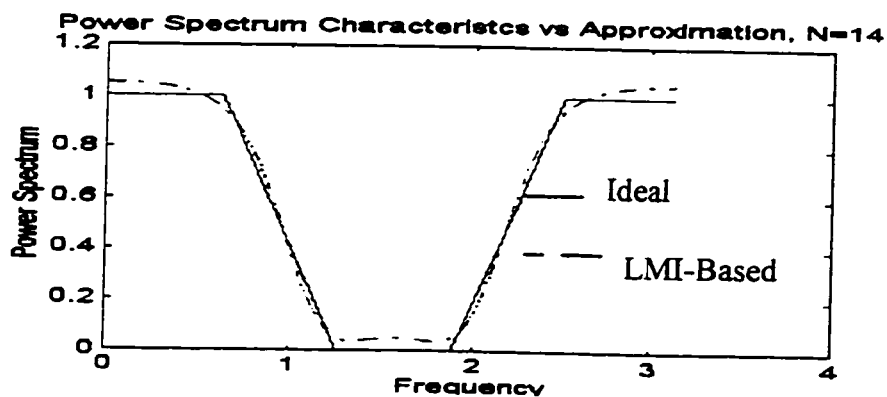


Figure 51 LMI-Based Approximation with $N=14$

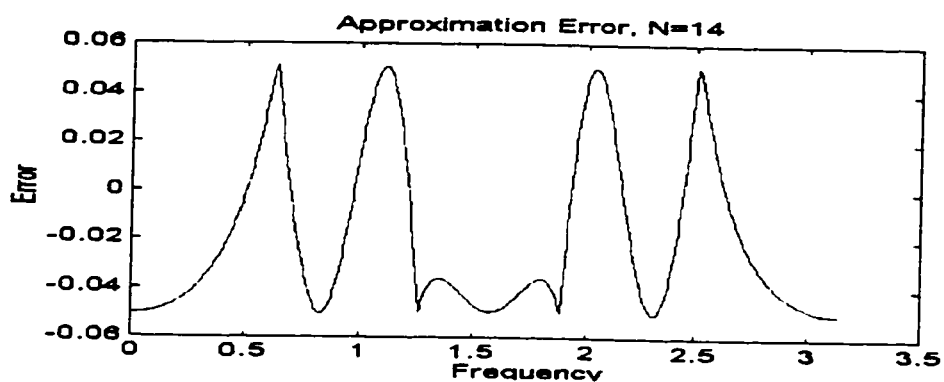


Figure 52 LMI-Based Approximation Error $N=14$

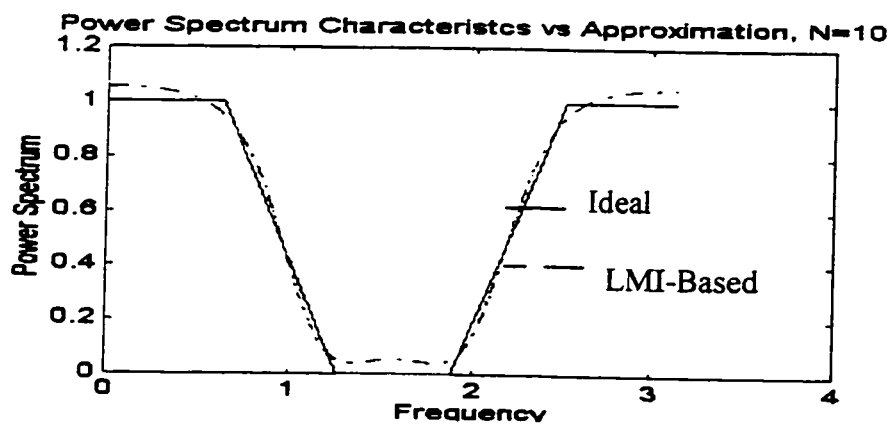


Figure 53 LMI-Based Approximation with $N=10$

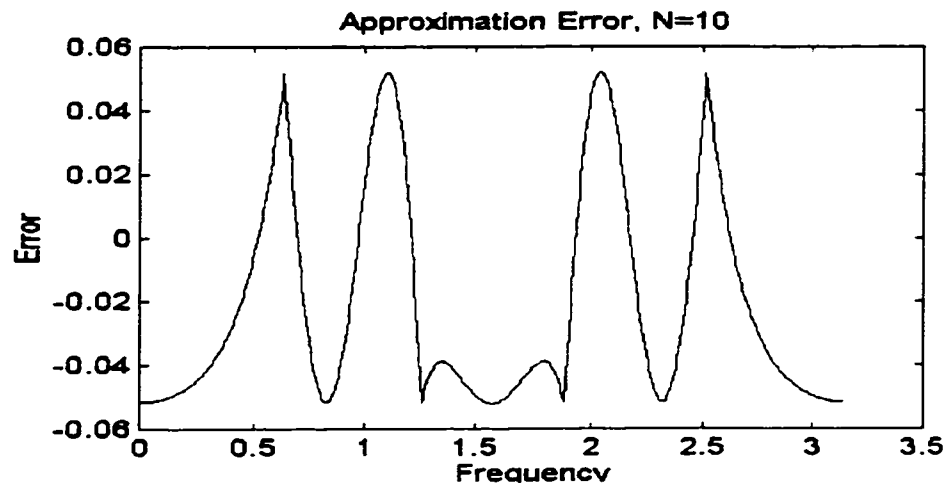


Figure 54 LMI-Based Approximation Error N=10

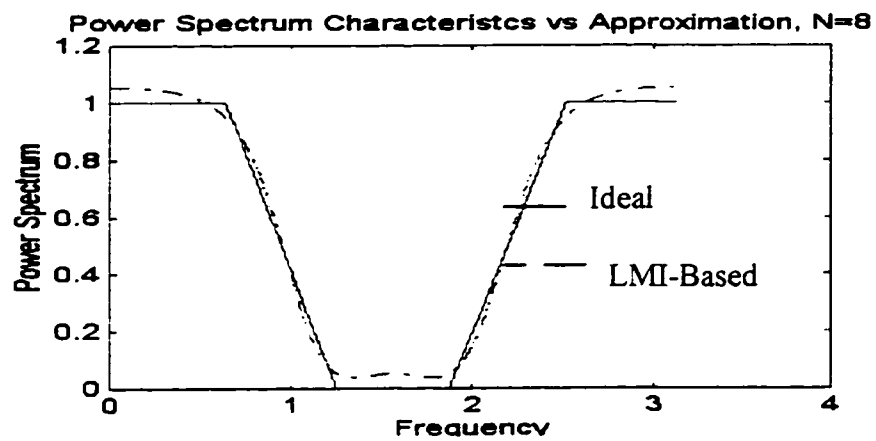


Figure 55 LMI-Based Approximation with N=8

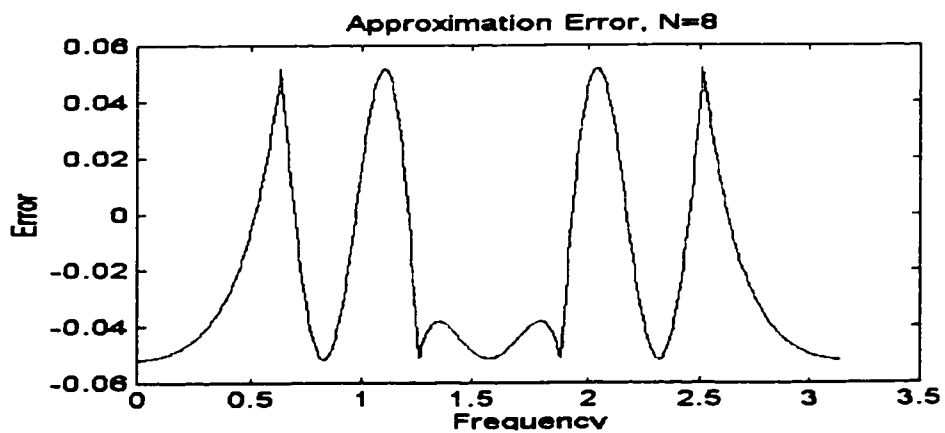


Figure 56 LIM-Based Approximation Error N=8

4.5. Model Reduction

The optimal LMI-Based filter design technique can easily be generalized to *Model Reduction Problem*. The following example will illustrate the *LMI-Based Model Reduction Algorithm*.

4.5.1 Example 7

Consider the following discrete time transfer function

$$G_d(z) = \frac{0.1201z^9 + 0.2773z^8 + 0.3874z^7 + 0.367z^6 + 0.1787z^5 - 0.0077z^4 - 0.2121z^3 - 0.2742z^2 - 0.2091z - 0.0973}{z^9 + 3.2015z^8 + 5.4004z^7 + 6.2184z^6 + 5.2442z^5 + 2.9391z^4 + 0.8021z^3 - 0.1041z^2 - 0.1328z - 0.0261}$$

Frequency characteristics of $G_d(j\omega)$ is given in Figure 57. It is required to find the

optimal $G(z) = \frac{n(z)}{d(z)}$ of order 4 that will solve the following problem.

$$\begin{aligned} \min_{n(z), d(z)} \quad & \gamma \\ \text{Subject To} \quad & \|(G_d(j\omega) - G(j\omega))\|_{\infty} < \gamma \quad \forall \omega \end{aligned}$$

where $W(\omega)$ is a weight function

Example 7 Objective: The objective of this example is to apply the LMI-Based Approximation technique to approximate a normal discrete time transfer function frequency characteristics with lower order function. The approximation model will be IIR.

Discussion and Results of Example 7: The fourth optimal approximation for a 9th order transfer function is as follows:

$$B_{\text{optimal}} = [-0.0095 \quad -0.2895 \quad -0.4259 \quad -0.5460 \quad -0.3664].$$

$$A_{\text{optimal}} = [1.0000 \quad 1.7176 \quad 1.9150 \quad 1.4232 \quad 0.7366].$$

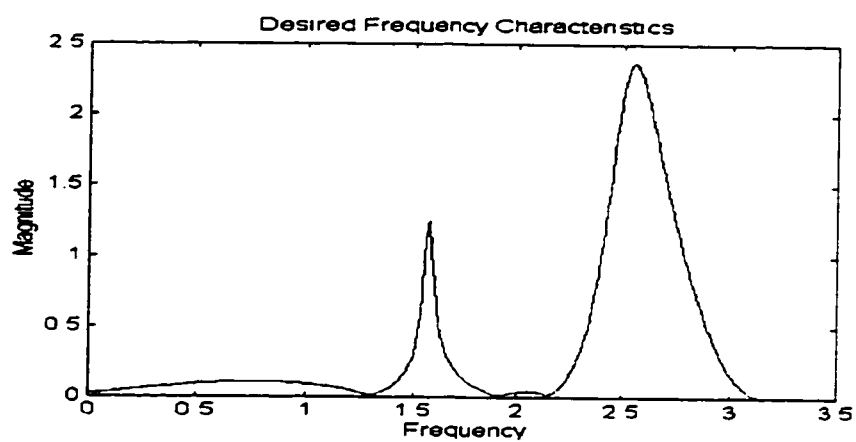


Figure 57 Desired Frequency Characteristics

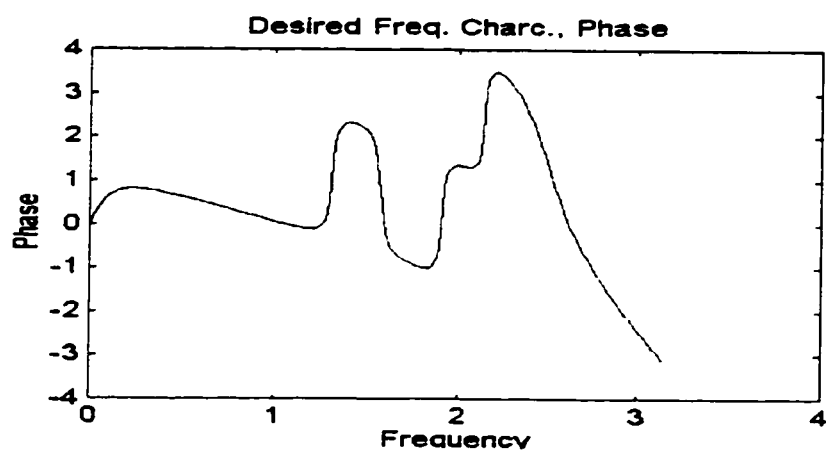


Figure 58 Desired Frequency Characteristics, Phase

The problem converged with 11 iterations for $d(\cdot)$. The problem used 300 equally spaced frequency points to reach an error of 0.5339. The theoretical lower bound of this error is 0.4402 which is the 4th Hankel Singular Value (HSV) of the system. The identification based technique in [27] produced for the same problem an error of 0.5393. Table 8 compares different approximation orders using the LMI-Based technique and the identification based technique.

	LMI-Based	Ident-Based	Lower Bound
8 th Order	0.0541	0.0542	0.0474
7 th Order	0.0664	0.0679	0.0631
6 th Order	0.0816	0.0850	0.0794
5 th Order	0.2670	0.2847	0.2336
4 th Order	0.5339	0.5393	0.4402
3 rd Order	0.9822	1.1093	0.6587

Table 8 Model Reduction Approximation Results

Figures of Example 7

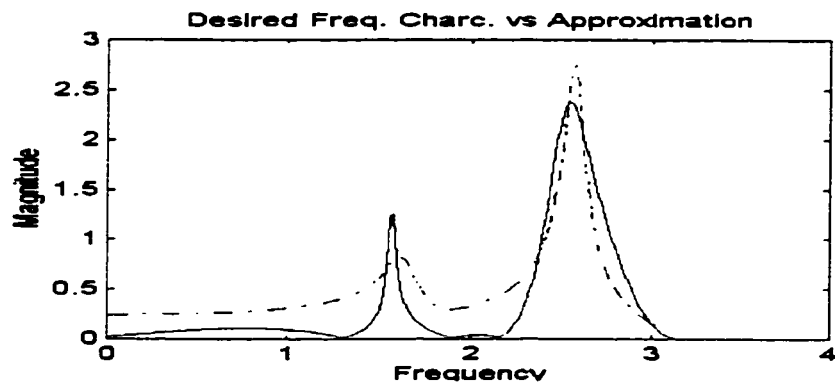


Figure 59 The desired vs the approximation

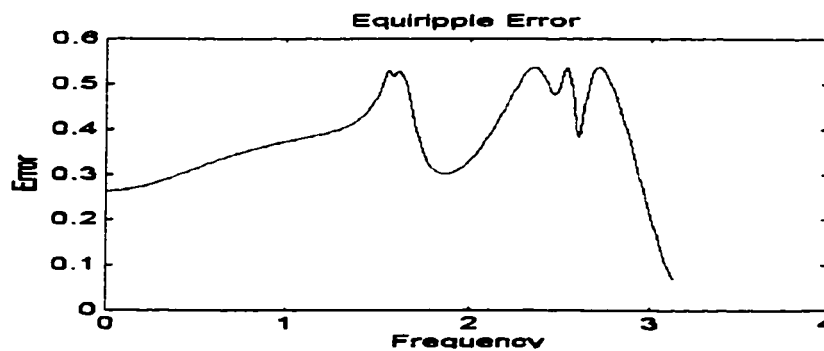


Figure 60 The Equiripple error behavior

CHAPTER 5

CONCLUSIONS, CONTRIBUTIONS AND FUTURE WORK

5.1 Conclusions

Based on the results obtained by applying the LMI-Based Optimal Filter Design to FIR, IIR and Power Spectrum models, following can be concluded.

- 1- The *LMI-Based Optimal Filter* design technique when applied with the FIR model always converges to the global optimal (in the L_∞ sense) if sufficient number of frequency points are selected within the range $[0, \pi]$. The result obtain is almost identical to the results obtained by *Remez Exchange Algorithm*. The more involved the desired frequency characteristics are, the bigger the frequency set is needed. However, the introduction of the *Frequency Selection Algorithm*, will enable the designer to start with a small set of equidistant frequencies and the algorithm itself will iterate for the frequencies corresponding to the error peaks to add them to the

next minimization run. The Frequency Selection Algorithm has been shown to reduce the convergence time tremendously.

- 2- The *LMI-Based Optimal Filter* design technique when applied with the IIR model, converges to an optimal (in the L_∞ sense) solution with equi-ripples behaving error. The approximation used to overcome the nonlinearity may cause divergence for some cases, though a counter example to the convergence case was not found in my limited simulation study. The optimal filter shows superior phase and magnitude error behavior when compared with the Yule Walker Least Squares Algorithm. Stability is an issue with IIR filters. Examples showed that the LMI-Based optimization technique may yield unstable optimal filter. Optimality can be maintained together with stability by replacing the unstable poles with their stable images and if the design requirements permits, by modifying the desired phase characteristics of the desired filter. Moreover, the *Frequency Selection Algorithm* was found to be extremely effective in reducing the number of LMIs solved to reach the optimal solution.
- 3- The *LMI-Based Optimal Power Spectrum Approximation* technique when applied with the FIR model converges to an optimal (in the L_∞ sense) solution with equi-ripples behaving error. The order of the FIR model chosen is reflected positively on the approximation error. Due to the symmetry imposed on the FIR model, the approximation will use only $\frac{1}{2}N$ number of coefficients (N is the approximation order) to characterize the approximate function. This is possible by characterizing it by its stable part only (roots are within the unit circle), depending on the fact that the other unstable part can be found by replacing z by $-z$.

- 4- The *LMI-Based Optimal Power Spectrum Approximation* technique when applied with the IIR model is observed to converge to an optimal (in the L_∞ sense) solution with equi-ripples behaving error. The performance of this approximation technique is superior when compared with the available techniques in literature.
- 5- The *LMI-Based Optimal Filter Design Algorithm* can be used to solve the *Optimal Model Reduction Problem*.

5.2 Contributions

1. Formulation of the FIR Optimal Filter Design Problem as Linear Objective Optimization Problem with LMI constraint, and development of the necessary software for solving it.
2. Formulation of the IIR Optimal Filter Design Problem as Linear Objective Optimization Problem with LMI constraint and with an iterative scheme to overcome the nonlinear term, and development of the necessary software for solving it.
3. Introduction of a Frequency Selection Algorithm that reduces the number of LMIs solved to reach the optimal solution.
4. Formulation of the FIR Optimal Power Spectrum Approximation Problem as Linear Objective Optimization Problem with LMI constraint, and development of the necessary software for solving it.

5. Formulation of the IIR Optimal Power Spectrum Approximation Problem as Linear Objective Optimization Problem with LMI constraint and with an iterative scheme to overcome the nonlinear term, and development of the necessary software for solving it.
6. Introduction of an LMI-Based Model Reduction Technique.

5.3 Future Work

- 1- Mapping the one dimensional LMI-Based optimization technique to the two dimensional case.
- 2- More in-depth theoretical analysis to the convergence of the LMI-Based Optimal IIR Filter Design.

Bibliography

- [1] X. Chen, Design of Optimal Digital Filters, Phd Dissertation, Rice University, Houston, Texas, April 1986.
- [2] H. El-Gamel, J. Soltis, M. Ahmadi, Order Reduction Technique using Chebychev polynomial and its application in digital filter design, IEE Proc. Circuits Devices Systems, Vol. 142, No.1, pp. 27-29, Feb. 1995.
- [3] R. D Strum, D. E Kirk, Discrete Systems and Digital Signal Processing, Addison-Wesley, 1989.
- [4] D. Burnside T. W. Parks, Optimal Design of FIR filters with the complex Chebyshev error criteria, IEEE Trans. on Signal Processing, Vol 43, No. 3 pp. 605-615, March 1995.
- [5] S. Wu, S. Boyd, L. Vandenberghe, FIR Filter Design via Semidefinite Programming, Proceedings of the 35th Conference on Decision and Control, Kobe, Japan, pp. 271-276, Dec. 1996.
- [6] A. G. Deczky, Synthesis of nonrecursive digital filters using minimum p-error criteria, IEEE Trans. Audio Electroacoust., AU-20, pp. 257-263, 1972.
- [7] A. T. Chottera and G. A. Jullien, A linear programming approach to recursive digital filter design with linear phase, IEEE Trans. Circuits Syst., CAS-29, pp. 139-149, 1982.
- [8] H. D. Helms, Digital filters with equiripple or minimax response, IEEE Trans. Audio Electroacoust., AU-19, pp. 87-94, 1971.
- [9] S. Ellacott and J. Williams, Characterization and computation of rational Chebychev Approximation in the complex plane, SIAM J. Numer. Anal., Vol 13, No. 3, pp. 310-323, 1976.
- [10] J. Williams, Characterization and computation of rational Chebychev approximation in the Complex Plane, SIAM J. Numer. Anal., Vol 16, No. 5, pp. 819-827, 1979.
- [11] M. H. Gutknecht and J. O. Smith and L.T. Trefethen, The Caratheodory-Fejer method for recursive digital filters design, IEEE Trans. Acoust., Speech, Signal Processing, ASSP-31, pp. 1417-1426, 1983.

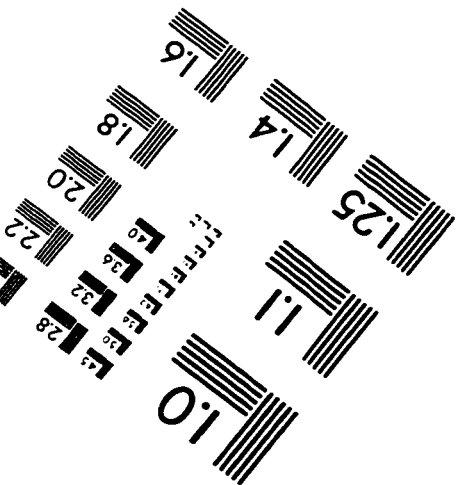
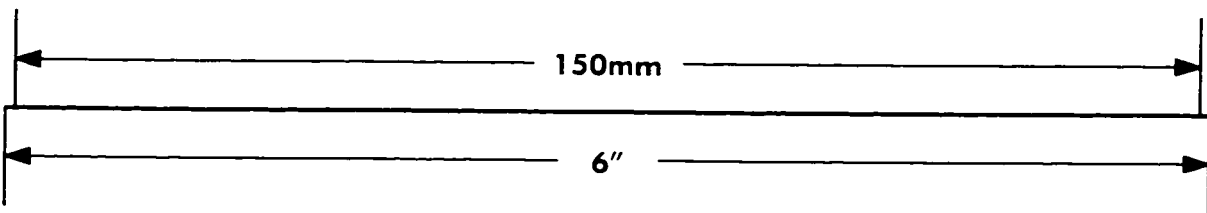
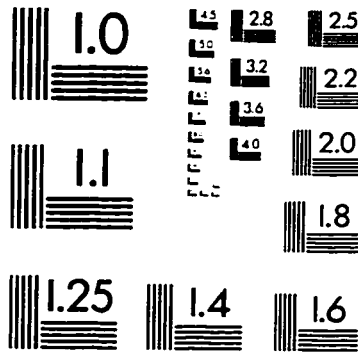
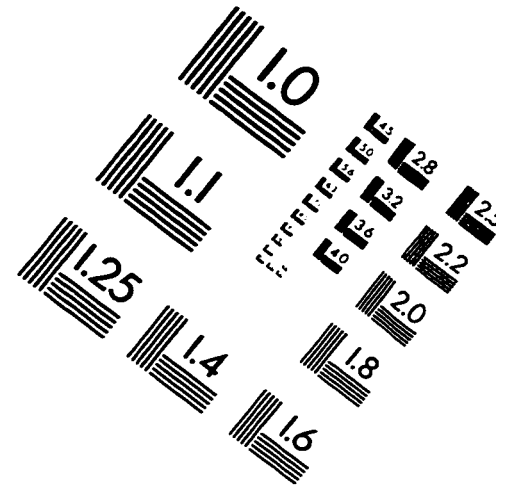
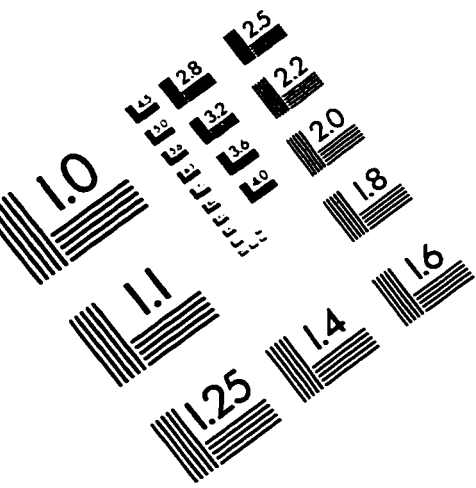
- [12] T. Kobayashi and S. R. Imai, Design of IIR digital filters with arbitrary log magnitude functions by WLS techniques. IEEE Trans. Acoust., Speech, Signal Processing, ASSP-38, pp. 247-252, 1990.
- [13] C. L. Lawson, Contribution to the theory of linear least maximum approximation, Ph.D. Thesis, University of California, 1961.
- [14] X. Chen and T. W. Parks, Design of IIR filters in the complex domain, IEEE Trans. Acoust., Speech, Signal Processing, ASSP-38, pp. 910-920, 1990.
- [15] Y. C. Lim, J.H. Lee, C. K. Chen and R.H. Yang, A weighted least squares algorithm for quasi- equiripple FIR and IIR digital filter design, IEEE Trans. Signal Processing, Vol 40, pp. 551-558, 1992.
- [16] J. H. Lee and C.K.Chen, Recursive digital filter design in the complex domain using an efficient method, Proc. 1992 IEEE International Symposium on Circuits and Systems Vol. 2, pp. 2429-2432, San Diego, 1992.
- [17] A. Antoniou, Improved Minmax Optimization Algorithms and their application in The Design of Recursive Digital Filteres, IEE Proceedings-G, Vol. 138, No. 6, pp. 724-730, Dec. 1991.
- [18] C. Charalambous, A Unified Review of Optimization, IEEE Tansactions MTT-22, pp. 289-300, 1974.
- [19] Rik Pintelon, Comments on Design of IIR Filters in The Complex Domain, IEEE Transactions on Signal Processing, Vol. 39, No. 6, pp. 1454-1455, June 1991.
- [20] Holford, Stephen, and Pan Agathoklis, The Use of Model Reduction Techniques for Designing IIR Filters with Linear Phase in the Passband, IEEE Transactions on Signal Processing, Vol.. 44, No. 10, pp. 2396-2404, October, 1996.
- [21] Beliczynski, B., J. Gryka, G. D. Cain and I. Kale, IIR Filter Design via Hankel-Norm Optimal Approximation of FIR Prototype Filters: A Streamlined Approach, Electronics Letters, Vol. 30, No. 4, pp. 292-293, 17th February 1994.
- [22] AlKhairy, Ashraf, On IIR Filter Design, IEEE International Symposium on Circuits and Systems, 1995, pp. 862-864.
- [23] A. Alkhairy, Design of Optimal IIR Filters with Arbitrary Magnitude, IEEE Transactions on Circuits and Systems-II: Analog and Digital Signal Processing, Vol 42, No. 9, pp. 618-620, Sept. 1995.

- [24] D. Kavranoglu and M. Bettayeb, Weighted L_∞ Norm Approximation with given Poles Using LMI Techniques and Applications, ECC 95, Rome, Italy, September 1995.
- [25] D. Kavranoglu and M. Bettayeb, An iterative Scheme for Rational H_∞ Approximation, ECC-TD 95, Istanbul, Turkey, August 1995.
- [26] D. Kavranoglu, Zeroth Order H_∞ Norm Approximation of Multivariable Systems, Numerical Functional Analysis and Optimization, Vol. 14(1&2), pp. 89-101, 1993.
- [27] D. Kavranoglu and M. S. Ahmed, H_∞ norm approximation by identification techniques, CDC 95, pp 796-801, New Orleans, USA, December 1995.
- [28] D. Kavranoglu and S. H. Al-Amer, A new frequency domain computational scheme for H_∞ norm system approximation, CDC-96, Kobe, Japan, pp. 4574-4579. December 1996
- [29] S. Boyd, L. El Ghaoui, E. Feron, and V. Balakrishnan, Linear Matrix Inequalities in Systems and Control Theory, SIAM, 1994.
- [30] Helmersson, A., Model Reduction Using LMIs, Proceedings of the 33rd Conference on Decision and Control, pp. 3217-3222, December 1994.
- [31] D. Kavranoglu and M. Bettayeb, Characterization and Computation of the Solution to the Optimal L_∞ Approximation Problem, IEEE Tran. Auto. Contr., Vol. 39, pp. 1899-1904, September 1994.
- [32] D. Kavranoglu, A Computational Scheme for H_∞ Model Reduction, IEEE Tran. Auto. Contr., Vol. 39, pp. 1447 - 1451, July, 1994.
- [33] Li, Huaizhong and Minyue Fu, An LMI Approach to Robust H_∞ Filtering for Linear Systems, Proceedings of the 34th Conference on Decision & Control, pp. 3608-3613, December, 1995.
- [34] P. Gahinet, A. Nemirovskii, Mahmoud Chilali, and A. Laub, LMI Control Toolbox, MATLAB[®] toolbox, December 1995.
- [35] J. G. Proakis and D. G. Manolakis, Digital Signal Processing, Maxwell-Macmillan, 1992.
- [36] Trefethen L. N., Chebyshev Approximation on the Unit Disk, Computational Aspects of Complex Analysis, 309-323, (Reidel Publishing Co. 1983).
- [37] D. Kavranoglu, S. Al-Amer and M. S. Ahmed , A New Technique for H_∞ Norm

System Approximation, Submitted to Systems & Control letters, April 1996.

- [38] D. Kavranoglu and M. Bettayeb, Characterization of the solution to the Optimal H_∞ Model Reduction Problem, Systems & Control Letters, Vol. 20, pp. 99-107, 1993.
- [39] D. Kavranoglu, S. Al-Amer and M. Bettayeb , A new identification based weighted H_∞ norm approximation scheme and its applications to controller reduction , To appear in IEE Proceeding, Part D: Control Theory and Application.
- [40] A. Edmond and J. William, Power Spectrum Reduction by Optimal Hankel Norm Approximation of the phase of the outer Spectral Factor, IEEE Trans. on Automatic Control, Vol. AC-30, No. 12, pp. 1192-1201, December 1985.
- [41] J. Juang, A. Edmond, A. Jonckheere. On computing the Spectral Radius of Hankel Plus Toeplitz Operator, IEEE Trans. On Automatic Control, Vol. 33, No. 11, pp. 1053-1059, November 1988.
- [42] A. V. Oppenheim and R. W. Schaffer, Discrete-Time Signal Processing, Prentice Hall, 1989.
- [43] Stonick, Virginia L. and S. Thomas Alexandar, Global Optimal IIR Filter Design and ARMA Estimation Using Homotopy Continuation Methods, IEEE International Conference on Acoustics, Speech, and Signal Processing, 1990, pp 1325-1328
- [44] Vandenberghe, Lieven and Venkataramanan Balakrishnan, Algorithms and Software Tools for LMI Problems in Control: An Overview, Proceedings of the 1996 IEEE International Symposium on Computer-Aided Control System Design, pp. 229-234, September, 1996.

IMAGE EVALUATION TEST TARGET (QA-3)



APPLIED IMAGE, Inc
1653 East Main Street
Rochester, NY 14609 USA
Phone: 716/482-0300
Fax: 716/288-5989

© 1993, Applied Image, Inc., All Rights Reserved

